

ผลของเมทัล โลจีนอีลาสโตเมอร์และความเร็วสกรูต่อพอลิโพรพิลีนคอมพาวนด์: สำนวนวิทยาและ
สมบัติกายภาพ



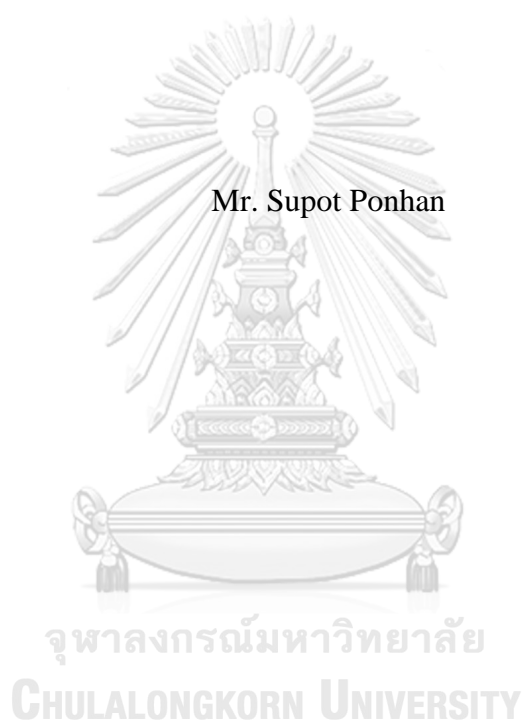
บทคัดย่อและแฟ้มข้อมูลฉบับเต็มของวิทยานิพนธ์ตั้งแต่ปีการศึกษา 2554 ที่ให้บริการในคลังปัญญาจุฬาฯ (CUIR)
เป็นแฟ้มข้อมูลของนิสิตเจ้าของวิทยานิพนธ์ ที่ส่งผ่านทางบัณฑิตวิทยาลัย

The abstract and full text of theses from the academic year 2011 in Chulalongkorn University Intellectual Repository (CUIR)
are the thesis authors' files submitted through the University Graduate School.

วิทยานิพนธ์นี้เป็นส่วนหนึ่งของการศึกษาตามหลักสูตรปริญญาวิทยาศาสตรมหาบัณฑิต
สาขาวิชาปิโตรเคมีและวิทยาศาสตร์พอลิเมอร์
คณะวิทยาศาสตร์ จุฬาลงกรณ์มหาวิทยาลัย
ปีการศึกษา 2560
ลิขสิทธิ์ของจุฬาลงกรณ์มหาวิทยาลัย

EFFECT OF METALLOCENE ELASTOMERS AND SCREW SPEED ON POLYPROPYLENE COMPOUNDS: MORPHOLOGICAL AND PHYSICAL PROPERTIES

Mr. Supot Ponhan



A Thesis Submitted in Partial Fulfillment of the Requirements
for the Degree of Master of Science Program in Petrochemistry and Polymer Science
Faculty of Science
Chulalongkorn University
Academic Year 2017
Copyright of Chulalongkorn University

สุพจน์ พลหาญ : ผลของเมทัลโลซีนอีลาสโตเมอร์และความเร็วสกรูต่อพอลิโพรพิลีนคอมพาวนด์: สันฐานวิทยาและสมบัติกายภาพ (EFFECT OF METALLOCENE ELASTOMERS AND SCREW SPEED ON POLYPROPYLENE COMPOUNDS: MORPHOLOGICAL AND PHYSICAL PROPERTIES) อ. ที่ปรึกษาวิทยานิพนธ์หลัก: ภัทรพรรณ ประศาสน์สารกิจ, 95 หน้า.

พอลิโพรพิลีน (PP) ซึ่งมีการใช้กันอย่างแพร่หลายในอุตสาหกรรมยานยนต์สามารถทดแทนพลาสติกวิศวกรรมและโลหะได้ เนื่องจากพอลิโพรพิลีนมีสมบัติเชิงกลที่โดดเด่น ง่ายต่อการขึ้นรูปและมีน้ำหนักเบา สำหรับชิ้นส่วนยานยนต์บางชนิด เช่น กันชนรถยนต์ ต้องมีสมบัติการทนแรงกระแทกสูง แต่สมบัตินี้เป็นข้อจำกัดของพอลิโพรพิลีน งานวิจัยนี้มีวัตถุประสงค์เพื่อปรับปรุงสมบัติการทนแรงกระแทก พร้อมทั้งรักษาความแข็งแรงและสมบัติทางกายภาพของพอลิโพรพิลีน โดยการผสม PP เมทัลโลซีนอีลาสโตเมอร์ (POE) ด้วยเครื่องอัดรีดแบบสกรูคู่ ในงานวิจัยนี้ศึกษาผลของชนิดพอลิโพรพิลีน ชนิดของเมทัลโลซีนอีลาสโตเมอร์ สัดส่วนการผสม PP/POE ต่อสมบัติกายภาพและสันฐานวิทยา จากผลการศึกษาพบว่า การทนแรงกระแทกของพอลิเมอร์ผสม PP/POE เพิ่มขึ้น เมื่อเพิ่มปริมาณของ POE พร้อมทั้งยังคงรักษาความแข็งแรงและสมบัติทางกายภาพของพอลิโพรพิลีนไว้ได้ในพอลิเมอร์ผสม PP/POE ที่สัดส่วน 70 ต่อ 30 โดยเฉพาะอย่างยิ่งเมื่อใช้ POE ชนิดยางเอทิลีนออกทีน (EOR) พบว่ามีการกระจายตัวของ POE ที่ดี ใน PP เมทริกซ์ นอกจากนี้เฟสต่อเนื่องของพอลิเมอร์เดี่ยว PP (H-PP) เป็นวัสดุความแข็งสามารถให้คุณสมบัติความแข็งสมมูลที่ดีขึ้นกว่าพอลิเมอร์ร่วม PP (C-PP) นอกจากนี้จากการศึกษาผลของความเร็วสกรู (400 ถึง 600 รอบต่อนาที) ต่อสมบัติกายภาพของพอลิเมอร์ผสม พบว่าความสามารถในการทนแรงกระแทกเพิ่มขึ้น เมื่อลดความเร็วสกรู สำหรับการศึกษาสันฐานวิทยาของพอลิเมอร์ผสม PP/POE พบว่าขนาดพื้นที่อนุภาคยางและอัตราส่วนยาวต่อกว้างของอนุภาคยางที่กระจายตัวบนพอลิโพรพิลีนส่งผลต่อสมบัติกายภาพของพอลิเมอร์ผสม พอลิเมอร์ผสม PP/POE ที่อัตราส่วน H-PP/EOR เท่ากับ 70/30 แสดงสมมูลที่ดีสำหรับสมบัติการทนแรงกระแทก ความแข็งแรง และรักษาสมบัติกายภาพ และมีศักยภาพใช้เป็นกันชนรถยนต์ได้

สาขาวิชา ปีโตรเคมีและวิทยาศาสตร์พอลิเมอร์ ลายมือชื่อนิติต

ปีการศึกษา 2560

ลายมือชื่อ อ.ที่ปรึกษาหลัก

ACKNOWLEDGEMENTS

The author wishes to express his deepest gratitude to his advisor, Professor Dr. Pattarapan Prasassarakich for her guidance, encouragement and helpful suggestion throughout this research. In addition, the author is also grateful to the to Associate Professor Dr. Prasert Reubroycharoen, Associate Professor Dr. Duangdao Aht-Ong, and Assistant Professor Dr. Suwadee Kongparakul, serving as the chairman and members of thesis committee, respectively, for their valuable suggestions and comments.

The author also wish to express thanks for kind support from SCG Chemicals Co.,LTD. and Program of Petrochemical and Polymer Science, Faculty of Science, Chulalongkorn University for their support with processing machine, testing equipment and materials.

Thanks go to his friends and everyone whose names are not mentioned here for their suggestions, assistances, advices concerning the experimental techniques and the encouragement during the period of this research. Finally, and most of all, the author would like to express his deep gratitude to his family for their tender, care, inspiration and encouragement.

CONTENTS

	Page
THAI ABSTRACT	iv
ENGLISH ABSTRACT.....	v
ACKNOWLEDGEMENTS.....	vi
CONTENTS.....	vii
LIST OF TABLES	x
LIST OF FIGURES	xii
LIST OF ABBREVIATIONS.....	xv
CHARTER I INTRODUCTION	16
1.1 The Purpose of the Investigation.....	16
1.2 Objective of the Research Work.....	17
1.3 Scope of the Investigation	17
1.4 Benefit of the Research Work	18
CHARTER II THEORY AND LITERATURE REVIEWS.....	19
2.1 Polypropylene.....	19
2.2 Classification of Polypropylene	21
2.2.1 Classification by stereo regularity	21
a) Isotactic polypropylene.....	22
b) Syndiotactic polypropylene	22
c) Atactic polypropylene.....	23
2.2.2 Classification by types.....	24
a) Homopolymer polypropylene.....	24
b) Copolymer polypropylene	24
c) Random copolymer polypropylene	25
2.3 Metallocene Elastomer	25
2.4 Melt-blending Technique	26
2.4.1 Twin screw extruder	26
2.4.2 Blend morphology	27
(i) Viscosity ratio.....	28

	Page
(ii) Effect of composition on the blend morphology	28
(iii) Blending and processing conditions	29
2.5 Literature Reviews.....	29
CHARTER III EXPERIMENTAL	35
3.1 Materials	35
3.2 Instruments	36
3.3 Compounding Preparation.....	36
3.4 Physical Properties Investigation	38
3.4.1 Melt flow index	38
3.4.2 Tensile properties	38
3.4.3 Flexural properties.....	39
3.4.4 Charpy impact strength	39
3.4.5 Izod impact strength	40
3.4.6 Shrinkage.....	40
3.4.7 Hardness	41
3.4.8 Heat distortion temperature	41
3.4.9 Extraction content by N-decane	41
3.4.10 Thermal properties.....	42
3.5 Morphological Investigation	42
CHARTER IV RESULTS AND DISCUSSIONS	44
4.1 Effect of polypropylene, metallocene elastomer type and blending ratio on physical properties of blends	44
4.1.1 Melt flow index	44
4.1.2 Impact properties	48
4.1.3 Tensile properties	52
4.1.4 Flexural properties.....	55
4.1.5 Shore-D hardness.....	57
4.1.6 Heat distortion temperature	58

	Page
4.1.7 Melting temperature (T_m), crystallization temperature (T_c) and %crystallinity (X_c).....	60
4.2 Effect of polypropylene, metallocene elastomer type and blending ratio on morphological properties of blends	63
4.3 Effect of screw speed on physical properties of blends	70
4.4 Effect of screw speed on morphological properties of blends	74
4.5 Cost estimation and Benchmarking of PP/POE blends.....	76
4.5.1 Cost estimation of blends	76
4.5.2 Benchmarking of PP/POE blends.....	76
CHARTER V CONCLUSIONS.....	79
5.1 Conclusions	79
5.2 Suggestion for Future Work.....	80
REFERENCES	81
APPENDIX.....	85
VITA.....	95

LIST OF TABLES

	Page
Table 3.1 Chemicals used in this study.....	35
Table 3.2 Instruments used in this study.....	36
Table 3.3 Composition of PP compounds (wt%).....	37
Table 4.1 Effect of PP and POE type and blending ratio on melt flow index of blends	45
Table 4.2 Effect of PP and POE type and blending ratio on extraction content of blends	46
Table 4.3 Effect of PP and POE type and blending ratio on impact properties of blends	50
Table 4.4 Effect of PP and POE type and blending ratio on tensile properties of blends	53
Table 4.5 Effect of PP and POE type and blending ratio on flexural properties of blends	56
Table 4.6 Effect of PP and POE type and blending ratio on shore-d hardness of blends	57
Table 4.7 Effect of PP and POE type and blending ratio on heat distortion temperature of blends.....	59
Table 4.8 Effect of PP, POE type and blending ratio on thermal properties of blends	61
Table 4.9 Average particle area of extracted rubber of blends	66
Table 4.10 Average aspect ratio of extracted rubber of blends	66
Table 4.11 Effect of PP and POE type and blending ratio on % shrinkage of blends	68
Table 4.12 Effect of screw speed on physical properties of blends.....	71

	Page
Table 4.13 Effect of screw speed on average particle area and aspect ratio of extracted rubber of H- PP/EOC30	75
Table 4.14 Summary estimated cost of PP/POE blends	76
Table 4.15 Benchmarking of PP/POE blends	77
Table A-1 Izod impact strength at 23°C of PP/POE blends.....	85
Table A-2 Izod impact strength at -30°C of PP/POE blends	86
Table A-3 Charpy impact strength at 23°C of PP/POE blends.....	87
Table A-4 Charpy impact strength at -30°C of PP/POE blends.....	88
Table A-5 Tensile strength of PP/POE blends.....	89
Table A-6 %Elongation at break of PP/POE blends.....	90
Table A-7 Tensile modulus of PP/POE blends.....	91
Table A-8 Flexural strength of PP/POE blends	92
Table A-9 Flexural modulus of PP/POE blends	93
Table A-10 Hardness (Shore-D) of PP/POE blends	94

LIST OF FIGURES

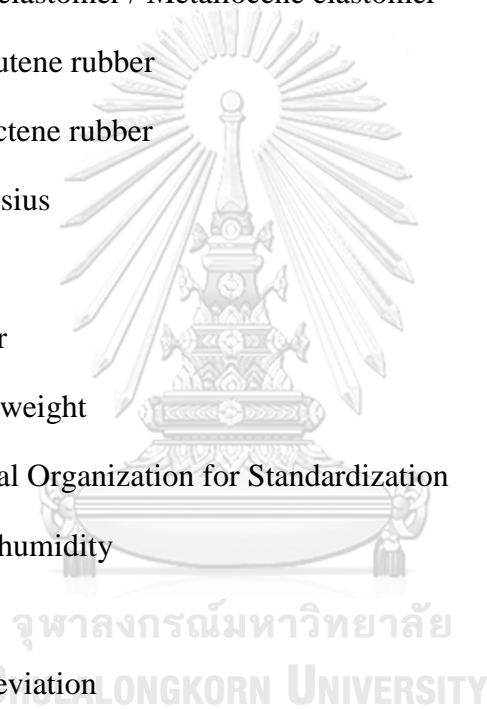
	Page
Figure 2.1 The reaction of propylene polymerization	20
Figure 2.2 Stereo regularity: (a) Isotactic, (b) Syndiotactic and (c) Atactic PP	21
Figure 2.3 Model of the helical chain of isotactic polypropylene in the crystalline state	22
Figure 2.4 Model of the helical chain of syndiotactic polypropylene in the crystalline state	23
Figure 2.5 Metallocene catalysts structure	26
Figure 2.6 Direction of the rotating of the screws; (a) Co-rotating, (b) Counter-rotating	27
Figure 2.7 The effect of POE content on MFI and impact strength of PP/POE compounds	30
Figure 2.8 TEM images of PP compounds; (a) EP/EOC, (b) EP/LLDPE, (c) EP/HDPE	31
Figure 2.9 SEM micrographs of PP/ethylene propylene random copolymer (EPR) blends; (a) 10 wt% of PBC-2, (b) 10 wt% of EOC, (c) 10 wt% of EBR	33
Figure 2.10 TEM images of ABS/Organoclay nanocomposites at different screw speeds; (a) 400 rpm, (b) 2000 rpm, (c) 4000 rpm	34
Figure 3.1 Tensile test specimen	38
Figure 3.2 Flexural test specimen	39
Figure 3.3 Charpy impact strength test specimen	39
Figure 3.4 Izod impact strength test specimen	40
Figure 3.5 shrinkage test specimen	40
Figure 3.6 heat distortion temperature test specimen	41

Figure 4.1 Effect of PP and POE type and blending ratio on melt flow index of blends.	45
Figure 4.2 Effect of PP and POE type and blending ratio on extraction content of blends.	47
Figure 4.3 The relation between extraction content and melt flow index of blends...	47
Figure 4.4 Effect of PP and POE type and blending ratio on impact properties of blends; (a) Charpy impact strength at 23°C, (b) Izod impact strength at 23°C, (c) Charpy impact strength at -30°C, (d) Izod impact strength at -30°C.	51
Figure 4.5 Effect of PP and POE type and blending ratio on tensile properties of blends; (a) Tensile strength, (b) % Elongation at break, (c) Tensile modulus.....	54
Figure 4.6 Effect of PP and POE type and blending ratio on flexural properties of blends; (a) Flexural strength, (b) Flexural modulus.....	56
Figure 4.7 Effect of PP and POE type and blending ratio on shore-d hardness of blends.	58
Figure 4.8 Effect of PP and POE type and blending ratio on heat distortion temperature of blends.....	59
Figure 4.9 Effect of PP and POE type and blending ratio on % crystallinity of blends.	61
Figure 4.10 DSC thermograms of the PP/POE blend; (a) H-PP/POE blend from the second heating scan, (b) C-PP/POE from the second heating scan, (c) C-PP/POE blend from the cooling scan, (d) C-PP/POE blend from the cooling scan. ...	62
Figure 4.11 SEM micrographs of H-PP/POE blends; (a) H-PP, (b) H-PP/EBR15, (c) H-PP/EOR15, (d) H-PP/EBR30, (e) H-PP/EOR30, (f) H-PP/EBR45, (g) H-PP/EOR45.....	64
Figure 4.12 SEM micrographs of H-PP/POE blends; (a) H-PP, (b) H-PP/EBR15, (c) H-PP/EOR15, (d) H-PP/EBR30, (e) H-PP/EOR30, (f) H-PP/EBR45, (g) H-PP/EOR45.....	65

Figure 4.13 Effect of PP and POE type and blending ratio on % shrinkage of blends; (a) Machine direction, MD and (b) Transverse machine direction, TD.....	68
Figure 4.14 The relation of shrinkage and average aspect ratio of extracted rubber of blends; (a) H-PP/EBR, (b) H-PP/EOR, (c) C-PP/EBR, (d) C-PP/EOR.	69
Figure 4.15 Effect of screw speed on physical properties of blends; (a) Melt flow index, (b) Impact strength at 23°C, (c) Impact strength at -30°C, (d) Tensile strength, (e) Elongation at break, (f) Tensile modulus.	72
Figure 4.16 Effect of screw speed on flexural properties of blends; (a) Flexural strength, (b) Flexural modulus.....	73
Figure 4.17 DSC thermograms of the H-PP/EOR30 blend; (a) T _m from the second heating scan, (b) T _c from the cooling scan.....	73
Figure 4.18 SEM micrographs of H-PP/EOR30 at various screw speed; (a) 400, (b) 500, (c) 600 rpm.....	74
Figure 4.19 Benchmarking of PP/POE blends.....	78

LIST OF ABBREVIATIONS

PP	: Polypropylene
H-PP	: Homopolymer polypropylene
C-PP	: Copolymer polypropylene
POE	: Polyolefin elastomer / Metallocene elastomer
EBR	: Ethylene butene rubber
EOR	: Ethylene octene rubber
°C	: Degree Celsius
g	: gram
µm	: Micrometer
wt%	: Percent by weight
ISO	: International Organization for Standardization
%RH	: %Relative humidity
Avg	: Average
SD	: Standard deviation
Min	: Minimum
Max	: Maximum



CHARTER I

INTRODUCTION

1.1 The Purpose of the Investigation

In automotive industry, plastic is used as a raw material for many automotive parts in both interior and exterior applications. From the assessment of the Plastics Manufacturers Association in Europe, the plastics usage is 105 kg approximately, 10% of the materials used in automobile production, the most plastic resin is Polypropylene (PP). Normally, PP can be used to produce automotive parts by increasing features with compounding and others material. PP compounds are used for a several parts such as bumper, instrumental panels and door trims, the various performance characteristics depends on performance requirements of the parts function [1]. A homopolymer PP is extensively employed as a substitute for engineering plastic and metals in car production due to outstanding mechanical properties, moldability, purity, high thermal stability, good chemical resistance, and especially its low density compared to other plastic materials which significantly contributes to fuel economy and reduced material costs [2].

Some automotive parts e.g. bumper require higher impact resistance which is the limited property of PP. To improve impact resistance or stiffness of materials, the additions of metallocene elastomers cloud improve impact resistance of PP by reducing glass transition temperature of PP compounds. A continuous phase PP was a stiffness material whereas the dispersed phase metallocene elastomer acted as impact modifier which provided the balancing stiffness-impact properties [2].

1.2 Objective of the Research Work

The objectives of this research are as follows:

1. To prepare the polypropylene compounds (Homopolymer, Copolymer) at various metallocene elastomer (EBR, EOR) contents (15, 30 and 45 wt%) and screw speed (400, 500 and 600 rpm) using twin screw extruder.
2. To investigate the physical properties and morphology of polypropylene compounds

1.3 Scope of the Investigation

The PP/metallocene elastomer blends were prepared at various blend ratios at 100:0, 85:15, 70:30 and 55:45 (wt%). Firstly, the effect of PP types, metallocene elastomer (POE) types and content on mechanical properties, morphology was studied. The experimental procedures were carried out as follows:

1. Survey literature and study the research work.
2. Prepare the PP/POE blends (H-PP/EBR, H-PP/EOR, C-PP/EBR and C-PP/EOR; H=Homopolymer PP and C=Copolymer PP) by using twin screw extruder at various blend ratios of PP and POE.
3. Prepare the test specimen of the PP/POE blends by using injection molding machine.
4. Investigate the mechanical properties of PP/POE blends.
5. Investigate the morphology of fracture test specimen by scanning electron microscope (SEM).
6. Investigate the physical and morphological properties of H-PP/EOR blends at 30% wt of EOR at various screw speed (400, 500 and 600 rpm).
7. Summarize the results.

1.4 Benefit of the Research Work

The new polypropylene compounds (PP/POE blends) could be applied in automotive industry (For Bumper parts with high melt flow index)



CHARTER II

THEORY AND LITERATURE REVIEWS

2.1 Polypropylene

Polypropylene (PP) is a thermoplastic addition polymer made from the combination of propylene monomers (Figure 2.1). PP is one of the most versatile and extensively used polymers in the world, used in a variety of applications to include packaging for consumer products, plastic parts for various industries including the automotive industry, special devices like living hinges, and textiles. Because of its excellent properties such as outstanding chemical and moisture resistance, good strength and stiffness, light weight, easy processing and relatively low price, PP has established itself as one of the most important polymers that has engineering plastic properties at commodity plastics prices [2].

Now, PP has a history over 60 years since its invention in 1954 and commercialization in 1957. It was first polymerized in 1951 by a pair of Phillips petroleum scientists named Paul Hogan and Robert Banks and later by Italian and German scientists Natta and Rehn. It became prominent extremely fast, as commercial production began barely three years after Italian chemist, Professor Giulio Natta, first polymerized it. Natta perfected and synthesized the first polypropylene resin in Spain in 1954, and the ability of polypropylene to crystallize created a lot of excitement. By 1957, its popularity had exploded and widespread commercial production began across Europe. Today it is one of the most commonly produced plastics in the world.

Structurally, PP is a vinyl polymer which is similar to polyethylene (PE), only that on every other carbon atom in the backbone chain has a methyl group attached to it [3]. PP can be produced from the propylene monomer by Ziegler-Natta polymerization or by metallocene catalysis polymerization.

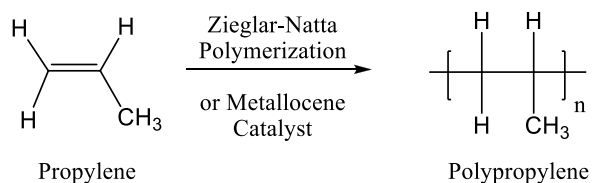


Figure 2.1 The reaction of propylene polymerization [2].

In the Ziegler-Natta polymerization, PP is synthesized by interaction with catalyst of titanium (IV) chloride and aluminum alkyl, such as triethyl aluminum. The polymerization process can be operated continuously with stereospecific, i.e. the insertion of asymmetric propylene monomers into the growing polymer chain in a given orientation is favored over all other possible orientations, leading to the production of isotactic and syndiotactic PP. Because these catalysts have more than one type of active site, they produce PP with broad molecular weight distribution (MWD) and non-uniform stereoregularity [4].

In contrast, metallocenes can be synthesized as single site-type catalysts to produce polymers with narrow MWD (with the theoretically predicted polydispersity index of two) and uniform stereoregularity. While it is very difficult to control the nature of the site types on conventional heterogeneous Ziegler-Natta catalysts, metallocene catalysts can be designed to synthesize PP with different chain microstructures. PP chains with atactic, isotactic, isotactic-stereoblock, atactic-stereoblock and hemiisotactic configurations can be produced with metallocene catalysts. It is also possible to synthesize PP chains that have optical activity by using only one of the enantiomeric forms of the catalyst [5].

Metallocene catalysts are organometallic coordination compounds in which one or two cyclopentadienyl rings or substituted cyclopentadienyl rings are π -bonded to a central transition metal atom. The most remarkable feature of these catalysts is that their molecular structure can be designed to create active center types to produce polymers with entirely novel properties. Metallocene catalyst systems can be conveniently divided into two categories. In the first category, an aluminoxane or an alkylaluminum, or a combination of aluminoxanes and alkylaluminums, are used to activate the metallocene catalyst. In the second category, an ion exchange compound,

comprising a cation and a noncoordinating anion, is combined with the metallocene catalyst. The cation reacts irreversibly with at least one of the metallocene ligands. The anion must be capable of stabilizing the transition metal cation complex and must be labile enough to be displaced by the monomer. The metallocene complex is therefore a cation associated with a stable anion.

2.2 Classification of Polypropylene

2.2.1 Classification by stereo regularity

Stereo regularity is called “tacticity” which is an important concept to understand the relation between the chemical structure and physical properties. The orientation of each methyl group (CH_3 -) relative to the methyl groups in neighboring monomer units greatly influences the crystalline properties of PP. PP has an asymmetric carbon atom, which determines the absolute configuration of the polymer structure. The tacticity of PP is classified into 3 types such as isotactic, syndiotactic, and atactic structures which are prepared by coordination polymerization (Figure 2.2) [6].

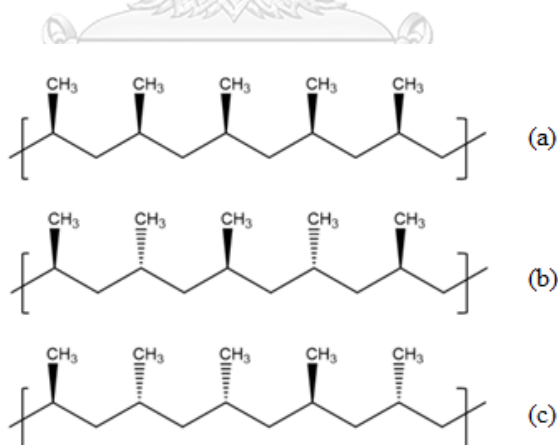


Figure 2.2 Stereo regularity: (a) Isotactic, (b) Syndiotactic and (c) Atactic PP [6].

a) Isotactic polypropylene

An isotactic polypropylene (*i*PP), the methyl groups of PP side chain are oriented in the same direction on the molecular backbone. It is produced by using a mixture catalyst system (TiCl_3 and AlR_2Cl) of Ziegler-Natta catalyst, which exhibits a high polymerization activity to produce *i*PP that is usually semi-crystalline and often forms a helix configuration (Figure 2.3) [6]. The melting point and glass-transition temperature are $160\text{-}166^\circ\text{C}$ and $\sim 20^\circ\text{C}$, respectively, which depend on the molar fraction of the meso (the same orientation of methyl group in neighbor unit) ratio. However, perfect *i*PP exhibits 176°C and -10°C , respectively. *i*PP is a rigidity material and has excellent heat resistance properties due to high crystal structure. Therefore, it is mostly used in various applications such as film, rigid packaging, technical parts, textiles etc.

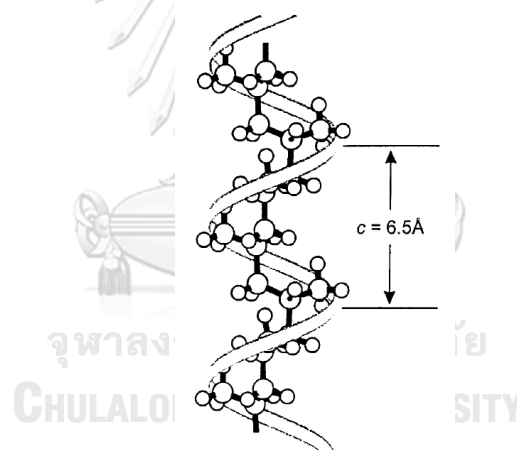


Figure 2.3 Model of the helical chain of isotactic polypropylene in the crystalline state [6].

b) Syndiotactic polypropylene

The syndiotactic form of PP was synthesized by using vanadium-based catalyst by Natta and coworkers. Syndiotactic polypropylene (*s*PP) is a semicrystalline and forms a helix configuration (Figure 2.4) like *i*PP but the absolute configuration of the asymmetric carbon atom is alternatively arranged in along the

chain (raceme) in *s*PP. In addition, metallocene catalysts is used to control the tacticity of the resulting PP as a function of ligand design that effectively provides syndiotactic structure. It was developed to a lower degree of crystallinity and, consequently, is more ductile at room temperature with greater impact strength [7]. In addition, the mechanical and thermal performances of *s*PP show a large scatter as a function of stereo and regioregularity of their chains that governs the crystallization [8]. Metallocene catalyzed *s*PP can be an elastomeric alternative to *i*PP for some applications, without significant differences in thermal properties required for a particular application [9]. *s*PP might have strong possibilities of being copolymerized with alpha-olefins of different lengths.

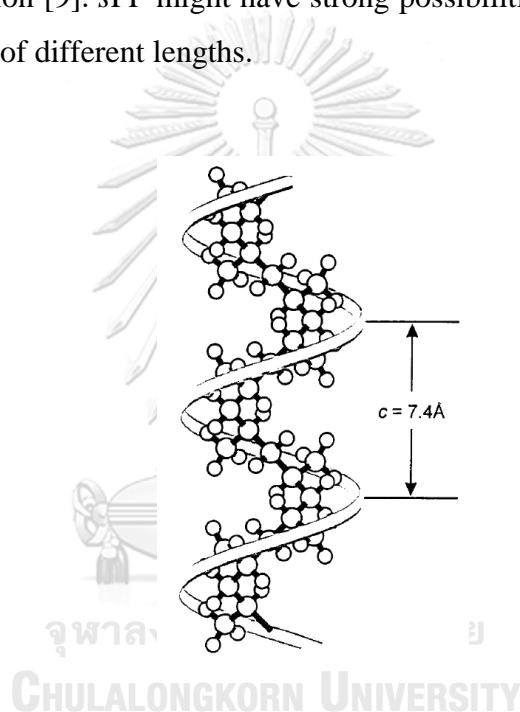


Figure 2.4 Model of the helical chain of syndiotactic polypropylene in the crystalline state [8].

c) Atactic polypropylene

In atactic polypropylene (*a*PP), the methyl groups are arranged randomly along the PP chain. The tacticity can be determined using ^{13}C -NMR (nuclear magnetic resonance) to analyze the meso and racemo ratio along the chain. *a*PP is prepared by radical polymerization with a low molecular weight because the hydrogen at the allyl position has a high reactivity.

2.2.2 Classification by types

There are three basic polypropylene types including homopolymers, block copolymers, and random Copolymers. The co-monomer is typically used with ethylene such as ethylene propylene rubber (EPR). It was added to PP homopolymer to increase its low temperature impact strength. Randomly polymerized ethylene added to PP homopolymer decreases the polymer crystallinity, lowers the melting point and makes the polymer more transparent. Although similar in many respects, each type exhibits distinct differences in both appearance and performance such as, homopolymers have the highest rigidity, copolymers have the highest impact resistance and random copolymers have the best transparency.

a) Homopolymer polypropylene

When a propylene monomer is polymerized into polypropylene, the product is called a homopolymer polypropylene (H-PP). H-PP is a thermoplastic resin produced through the polymerization of propylene with Ziegler-Natta catalysts. It can be used in different processing technologies, such as injection molding, blow molding, film, fiber, sheet extrusion and thermoforming. H-PP can be referred to as the state of the polypropylene material, which offers a high strength to weight ratio and is stiffer and stronger than copolymer, this combined with good chemical resistance and weldability allows this material to be used in many corrosion resistance structure.

b) Copolymer polypropylene

Copolymer polypropylene (C-PP) or block copolymer has co-monomer units arranged in blocks (that is, in a regular pattern) and contain anywhere between 5% to 15% ethylene by using Ziegler Natta catalysts [10]. Ethylene improves certain properties, like impact resistance. Their synthesis consists of a heterophasic amorphous structure inside a semi-crystalline homopolymer PP matrix. C-PP is a bit softer tougher and more durable than H-PP. In addition, it tends to have better stress crack resistance and low temperature toughness than homopolymer at the

expense of quite small reductions in other properties. This allows PP to be used as an engineering plastic, competing with materials such as acrylonitrile butadiene styrene (ABS).

c) Random copolymer polypropylene

Random copolymer polypropylene (R-PP) is opposed to block copolymer polypropylene which is incorporated co-monomer units arranged in irregular or random patterns along the polypropylene molecule. They are usually incorporated with anywhere between 1% to 7% ethylene and are selected where a lower melting point, more flexibility, and enhanced clarity are advantageous [11] [12]. R-PP is used in a wide range of application including high clarity or transparency packaging, injection molding, blown molding, extrusion casting, piping, and thermoforming. Conventional Ziegler-Natta catalysts limit the production of R-PP to relatively low levels of an ethylene monomer. Low-melting random copolymers are difficult to produce in a conventional polypropylene industrial process because the sticky nature of the resin causes fusion and blockage during the polymerization process.

2.3 Metallocene Elastomer

Metallocene elastomer or polyolefin elastomer is a relatively new class of polymers and a one of the fastest growing synthetic polymers that is a copolymer of ethylene and another alpha-olefin co-monomer such as butene or octene which synthesized by metallocene catalyst. Increasing the comonomer (butene or octane) content will produce polymers with higher elasticity as theco-monomer incorporation disrupts the polyethylene crystallinity. Furthermore, the molecular weight of the copolymer determines its processing characteristics and end-use performance properties with higher molecular weights providing enhanced polymer toughness. Ethylene propylene rubbers (EPR or EPDM) are the most popular polyolefin elastomer materials because they are an excellent impact modifier for plastics, and offer unique performance capabilities for compounded products [13] [14]. Recently,

EPR is compounded with PP as a leading material for automotive exterior and interior applications due to high impact resistance property.

Polyolefin elastomers are produced using refined metallocene catalyst often referred to as single-site or constrained geometry catalysts. These catalysts have a constrained transition metal (generally a Group 4B metal such as Ti, Zr, or Hf) sandwiched between one or more cyclopentadienyl ring structures to form a sterically hindered polymerization site [15] (Figure 2.5). This unique catalyst provides a single polymerization site instead of the multiple sites of conventional catalysts and provides the capability to tailor the molecular architecture of ethylene copolymers.

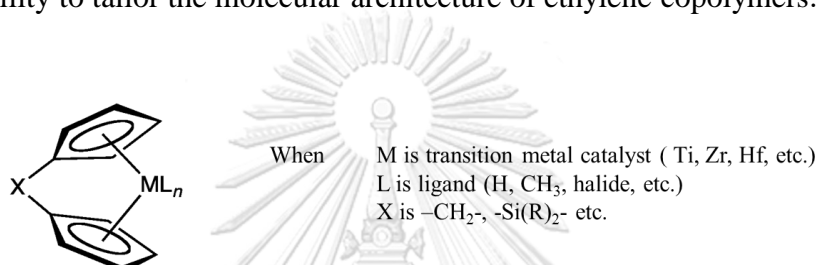


Figure 2.5 Metallocene catalysts structure [15].

2.4 Melt-blending Technique

2.4.1 Twin screw extruder

Twin screw extrusion is used extensively for mixing, compounding, or reacting polymeric materials due to their continuous operation, versatility, and effective mixing action. It offers several advantages over single screw extruder such as better feeding, mixing, and control of the residence times and stock temperature because flexibility of twin screw extrusion equipment allows this operation to be designed specifically for the formulation being processed. There are various types of twin-screw extruders available commercially. They differ in their design and operating principles, thus in their abilities for distributive and dispersive mixing and hence their application areas. The available twin-screw extruders can be classified as co-rotating and counter-rotating, on the basis of the direction of the rotating of the screws [16] (Figure 2.6).

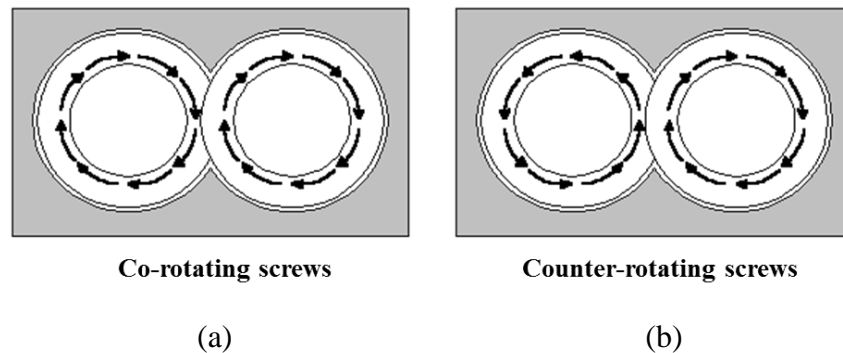


Figure 2.6 Direction of the rotating of the screws; (a) Co-rotating, (b) Counter-rotating [16].

The counter-rotating extruders can be classified in terms of the degree of intermeshing of the screws, ranging from fully intermeshed, where the flight of one screw fits tightly into the channel of the other screw, to non-intermeshing "tangential", where the two screws rotate freely in their barrel sections.

The co-rotating twin screw extruders are not produced in the non-intermeshing mode. Further differences can be found in the form of screw flight. Co-rotating designs, for example, may have rounded or so-called self-wiping screw flights, which have large channel clearances across the intermeshing zone, or trapezoidal shaped channels and flights with more restricted interchannel flow. This can have important implications with regard to their positive conveying efficiency and the nature of mixing between the screws. Trapezoidal shaped screws are generally more effective in both these respects [17].

2.4.2 Blend morphology

Since PP and EPR are immiscible, its blends tend to phase-separate and two-phase systems are obtained where EPR forms a discontinuous phase within a continuous PP matrix. The physical behaviors as well as the final use-properties of the blends are related to the blend morphology, which is affected by many factors. Apart from the nature of components (both molecular structure and chemical nature), viscosity ratio of plastic and rubber (or elastomer), blend composition and level of

dispersion are major factors controlling the blend morphology. The dispersion level is in turn affected by the technique and conditions of compounding.

(i) Viscosity ratio

The viscosity ratio has been shown to be one of the most critical variables in controlling blend morphology. The size and size distribution of the disperse phase were found to be determined mainly by the value of viscosity ratio. Generally matching the viscosities results in a fine morphology. There have been extensive studies on the rheological behavior of mechanical blends of molten polymers such as iPP/EPDM system that there was a linear relationship between the number average diameter of the minor phase (EPDM) and the viscosity ratio. The particle size increased with increasing viscosity ratio. Fine dispersions could be achieved if the ethylene content of EPDM is low and the viscosity ratio value is near unity. The melt viscosity values of the blends were found to be lower than the mean value of the simple components. When the amount of rubber in the blend increased (80 EPR/20 PP) [18], the viscosity ratio became less important in determining the state of dispersion.

(ii) Effect of composition on the blend morphology

The changes in blend composition can influence the state of dispersion of the phases in the blend via the changes in viscosity of polymer melts. For PP/EPDM blends, a continuous PP phase was obtained at low EPDM content (less than 25-30 vol%) and continuous elastomer phase seen at high EPDM content (higher than 80 vol%) with a transitional structure is observed in between [19]. In addition, the phase structures of blending between PP and EPR change in the composition range from 60/40 to 50/50 of PP/EPR in the case whereas the viscosity of PP is more than that of EPR and from 50/50 to 60/40 in case of viscosity of PP is lower than that of EPR [20]. It means that the size of elastomeric particles increases by increasing the EPR concentration. Further increase in the elastomer concentration,

the elastomeric phase becomes continuous and the system has a structure comprising physically interpenetrating networks.

(iii) Blending and processing conditions

Both processing equipment and compounding conditions used, such as type of mixing device, screw configuration, rotor speed, mixing time and energy input, play an important role in determining the morphology of polymer blends. For examples, the processing variables in 70/30 (by weight) PP/EPDM blends on a co-rotating twin screw extruder [21]. Increasing the screw speed also resulted in more uniform EPDM distribution because the material was exposed to more shearing. On the other hand, increasing the material throughput produced a coarsening of the EPDM structure [22].

2.5 Literature Reviews

Liu *et al.* [23] studied of the mechanical and morphological properties of toughened polypropylene blends for automobile bumpers. The polyolefin elastomer (POE, ethylene octene copolymer), 0-20 wt% and high density polyethylene (HDPE), 0-5wt% were added in order to improve impact properties for PP copolymer and toughness of PP/POE compounds, respectively. The POE content (wt%) increased with increasing impact properties of PP as shown in Figure 2.7. In addition, HDPE improved the toughness properties of PP/POE compounds. On the other hand, melt flow index of PP and PP/POE compounds, crystallinity degree (XC) of the PP/POE compounds are also decreased with increasing the POE and HDPE content. As morphological properties, the particles size of the dispersed became larger when content of POE was increased.

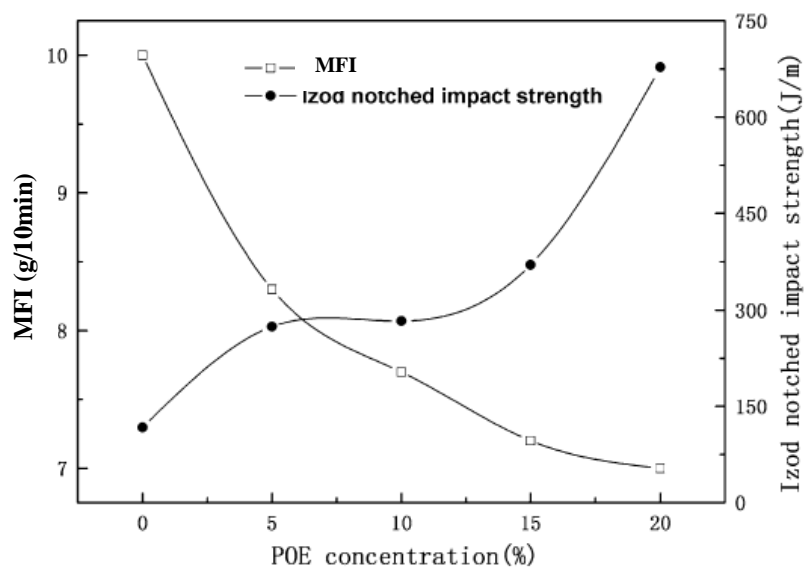


Figure 2.7 The effect of POE content on MFI and impact strength of PP/POE compounds [23].

Hainan *et al.* [24] studied the Influence of phase morphology and crystalline structure on the toughness of rubber-toughened isotactic polypropylene blends. Moreover, the effect of specimen preparation by compression and injection molding were investigated. As rubber content, POE (0-35 wt%) increased impact resistance improved while tensile strength decreased. However, the low concentration of nucleating agent at 0.05wt% (PP/POE10/0.05-I) assisted to balance impact resistant and tensile strength properties of PP/POE blends in comparison with 0.5wt% (PP/POE10/0.5-I). For different specimen preparation method, a particle size of rubber by compression molding (PP/POE10/0.05-C, PP/POE10/0.5-C) was significant higher than injection molding (PP/POE10/0.05-I, PP/POE10/0.5-I). Furthermore, the rubber of PP/POE blends was elongated on flow direction of injection molding which significant increased impact resistance properties.

Cornelia *et al* [25] studied the Interaction between rheology and morphology of polypropylene/polyethylene blends as models for high-impact propylene–ethylene copolymers. Homopolymer polypropylene (H-PP) and propylene ethylene random copolymer (EP) were main matrix. The content of dispersed phase (5–30 wt%) of ethylene octene copolymer (EOC), linear low density polyethylene (LLDPE), and

high density polyethylene (HDPE) were investigated. The type of dispersed and matrix phase affected the compatibility and degree of interaction between matrix and dispersed phase. Furthermore, EP showed higher compatibility between dispersed phases than PP. The particles size decreased when changing the dispersed phase from EOC (RPEO20) to LLDPE (RPHD20), it can be explained by low interfacial tension result. The good compatibility cloud improves the mechanical and optical properties. (Figure 2.8)

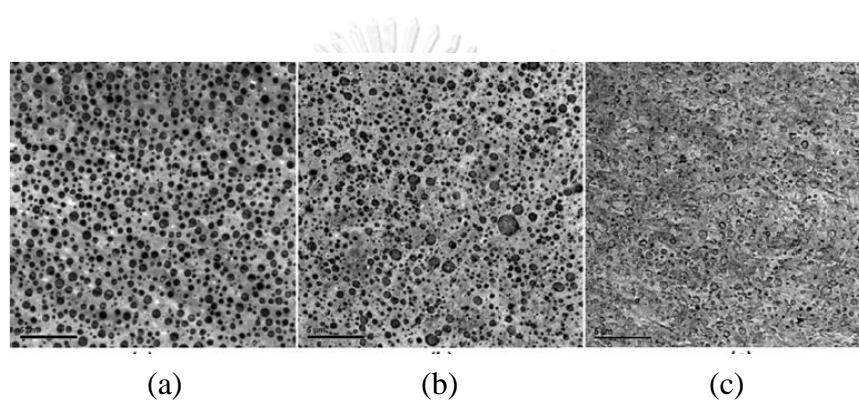


Figure 2.8 TEM images of PP compounds; (a) EP/EOC, (b) EP/LLDPE, (c) EP/HDPE [25].

Cornelia *et al* [26] studied the relation between composition and mechanical properties of polypropylene/polyethylene blends as models for high-impact polypropylene-ethylene copolymers. The blend of high-density polyethylene (HDPE), linear low density polyethylene (LLDPE) and ethylene octene copolymer (EOC) in homopolymer polypropylene (H-PP) and propylene ethylene random copolymer (EP) were investigated. EP/EOC blends showed the highest toughness properties in comparison with HDPE and LLDPE. On the other hand, the modulus of PP matrix/HDPE blends showed the better than LLDPE and EOC. Thus, the polymer matrix, content and type of modifier affected the mechanical properties.

Grestenberger *et al* [27] studied the basic correlations between EPR-design and shrinkage of polypropylene/ethylene-propylene rubber (PP/EPR) blends for the automotive industry. From the morphology determined by scanning electron

microscopy (SEM), the increased particle size and decreased in the particle aspect ratio resulted from the increasing the molecular weight of EPR. The coarsening of the phase morphology affects to increase shrinkage and coefficient of linear thermal expansion (CLTE) with the molecular weight of the EPR phase. Comparison of adding the nucleated and non-nucleated materials, the increasing shrinkage on transverse flow direction was observed which affected from high crystallinity of the nucleated sample. Meanwhile, the high molding shrinkage from nucleation of PP was occurred in the same processing condition that is inverse for the CLTE.

Sedigheh *et al* [28] studied the effects of blending sequence on morphology and mechanical properties of polypropylene (PP)/ethylene-octene copolymer (EOC)/clay nanocomposites. The maleated grafted-polypropylene (PP-g-MA) and maleated grafted- EOC (EOC-g-MA) were compatibiliser. The blending of all composition gave the highest impact resistance due to good dispersion of clay in PP and EOC matrix. In addition, the better dispersion of clay in PP was observed when using EOC-g-MA as compatibiliser. However, there is no significant difference on flexural modulus, tensile strength and tensile modulus of PP/EOC-g-MA blends.

Wu *et al* [29] studied the mechanical properties, morphology and crystallization behavior of polypropylene (PP)/elastomer (POE) /talc composites. The tensile strength, storage modulus, heat deflection temperatures and %crystallinity increased while elongation and izod impact strength were decreased with decreasing particle size of talc blends. In addition, the addition of POE, elongation at break and impact properties were increased. Conversely, tensile strength, flexural properties, storage modulus and heat deflection temperatures decreased compared with neat PP. For effect of MFI of POE on mechanical properties, the difference of MFI did not affect the impact properties of PP/POE blends. Thus, to improve and balance the mechanical properties and thermomechanical properties, PP/POE/talc blends was studied. The mechanical properties and thermomechanical properties of PP/POE/talc was higher than those of PP and PP/POE blends.

Camille *et al* [30] studied the elaboration of low viscosity and high impact polypropylene blends through reactive extrusion. The viscosity of polymer blends was significantly decreased when using the large difference a melt flow index of PP, mechanical properties and impact resistance were dramatically decreased. Higher

molecular weight or viscosity of the thermoplastic elastomer, impact strength and elongation at break were enhanced in comparison with lower molecular weight or viscosity. In addition, the miscibility of PBCs with PP, fine dispersion was observed by SEM. On the other hand, the relative immiscibility of EOC and EBR, larger particles was found (Figure 2.9), this phenomenon led to weak interface and lower impact enhancement.

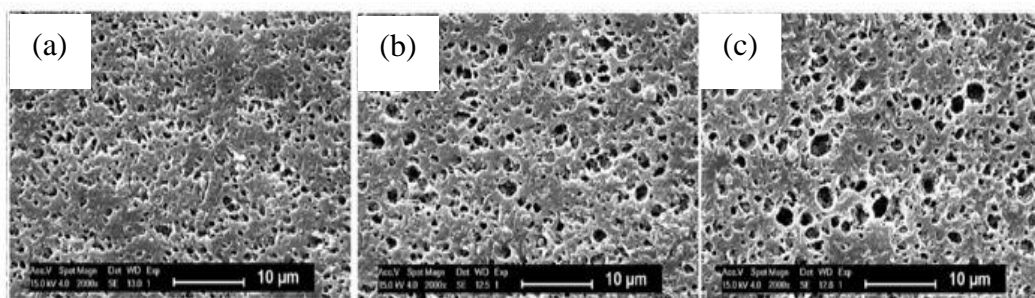


Figure 2.9 SEM micrographs of PP/ethylene propylene random copolymer (EPR) blends; (a) 10 wt% of PBC-2, (b) 10 wt% of EOC, (c) 10 wt% of EBR [30].

Azadeh *et al* [31] studied the effect of ultra-high speed twin screw extrusion on ABS/organoclay nanocomposite blend properties. The increase in screw speed (400 – 4000 rpm), decrease the impact strength while the ultimate tensile strength and tensile module were increased more up to screw speeds of 2000 rpm, and then decreased consistent with the result of XRD and TEM that the better intercalation and exfoliation were observed at higher screw speeds up to 2000 rpm. (Figure 2.10)

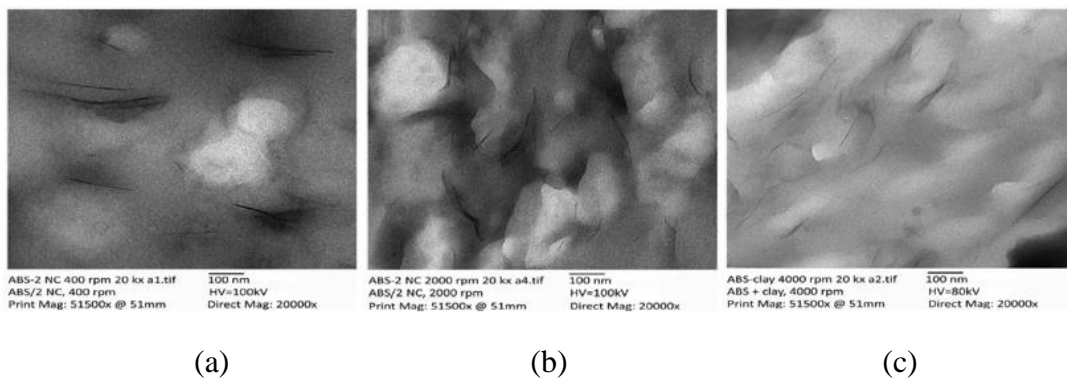


Figure 2.10 TEM images of ABS/Organoclay nanocomposites at different screw speeds; (a) 400 rpm, (b) 2000 rpm, (c) 4000 rpm [31].



CHARTER III

EXPERIMENTAL

3.1 Materials

Table 3.1 Chemicals used in this study

Chemicals	Function	Supplier
Homopolymer polypropylene (H-PP)	Base polymer	Thai Polypropylene Co., Ltd. (SCG Chemicals Group)
Copolymer polypropylene; (C-PP, Ethylene content 10%)	Base polymer	Thai Polypropylene Co., Ltd. (SCG Chemicals Group)
Ethylene butene rubber; EBR (%Crystallinity = 13)	Metallocene elastomer	Dow Chemical Thailand Ltd.
Ethylene octene rubber; EOR (%Crystallinity = 19)	Metallocene elastomer	Dow Chemical Thailand Ltd.
<i>n</i> -Decane	Solvent	Merck Co., Ltd.
<i>n</i> -Heptane	Solvent	RCI LABSCAN CO.,LTD

3.2 Instruments

Table 3.2 Instruments used in this study

Instruments	Manufacturer
Auto fine coater	Jeol Ltd.
Charpy impact machine	Toyo Seiki Seisaku-sho, Ltd.
Differential scanning calorimetry	Mettler-Toledo International Inc.
Durometer	Mitutoyo Corporation.
Heat deflection tester	Coesfeld GmbH & Co. KG
Injection molding machine	Fanuc thai limited.
Izod impact machine	Yasuda Seki Seisakusho Ltd.
Melt flow indexer	Dynisco Ltd.
Profile projector	Nikon Corporation.
Scanning electron microscope (SEM)	Jeol Ltd.
Twin screw extruder	Labtech Engineering Company Ltd.
Universal testing machine	Instron (Thailand) Co., Ltd.

3.3 Compounding Preparation

Homopolymer and copolymer polypropylene sample were used as base polymer. The PP/POE blends were prepared according to the formulation in Table 3.3. All components were mixed by using thumble blender for 10 min and kept in a plastic bag before feeding into the extruder hopper for compounding. The samples were compounded using a twin screw extruder ($D = 26$ mm, $L/D = 40$), with vacuum degassing and temperature profile from hopper to die; 100, 190, 190, 200, 200, 220, 220, 220, 220, and 210°C, screw speed; 600 rpm and throughput rate; 45 kg/h. After extrusion from die, the strands were cooled in water and pelletized. Polypropylene compound pellet were mixed in silo for 30 min and filled in a plastic bag before preparation of test specimen.

In addition, homopolymer polypropylene (H-PP)/EOR blend at 30 wt% of EOR content was prepared at various screw speed; 400, 500 and 600 rpm using same preparation process and processing parameter as above mentioned.

Table 3.3 Composition of PP compounds (wt%)

Formulation Name	Material	Content	Metallocene	
			elastomer type	Content
H-PP	Homopolymer polypropylene	100	-	0
H-PP/EBR15	Homopolymer polypropylene	85	EBR	15
H-PP/EBR30	Homopolymer polypropylene	70	EBR	30
H-PP/EBR45	Homopolymer polypropylene	55	EBR	45
H-PP/EOR15	Homopolymer polypropylene	85	EOR	15
H-PP/EOR30	Homopolymer polypropylene	70	EOR	30
H-PP/EOR45	Homopolymer polypropylene	55	EOR	45
C-PP	Copolymer polypropylene	100	-	0
C-PP/EBR15	Copolymer polypropylene	85	EBR	15
C-PP/EBR30	Copolymer polypropylene	70	EBR	30
C-PP/EBR45	Copolymer polypropylene	55	EBR	45
C-PP/EOR15	Copolymer polypropylene	85	EOR	15
C-PP/EOR30	Copolymer polypropylene	70	EOR	30
C-PP/EOR45	Copolymer polypropylene	55	EOR	45

For test specimen preparation, the test specimens were injection molded at temperature profile from hopper to nozzle; 190, 200, 200 and 200°C, mold temperature; 40°C and injection velocity was 200±20 mm/sec. After molding, the specimens were kept in controlled room at 23 ± 2 °C and 50 ± 5 %RH for 40 h according to ISO 1873-2.

3.4 Physical Properties Investigation

3.4.1 Melt flow index

The melt flow indexes of samples were determined according to ISO 1133-1:2011 (Procedure A). Melt flow index was measured using melt flow indexer (Dynisco, D4003HV) at temperature of $230 \pm 2^\circ\text{C}$, load of 2.16 kg and cutting time of 40 s. An average of 2 measurements was reported as a representative value in g/10/min.

3.4.2 Tensile properties

The tensile properties of test specimen were determined according to ISO 527-1:2012. Tensile properties was measured using universal testing machine (INSTRON, 5566) with cross head speed of 50 mm/min at the test condition of $23 \pm 2^\circ\text{C}$ and $50 \pm 5\% \text{RH}$. The width and thickness of test specimen were measured by using digital micrometer with the resolution of 0.001 mm. An average of five specimens was reported as a representative value. The tensile strength (TS.) and elongation at break (EB.) were recorded and determined as an average. The tensile specimen is shown in Figure 3.1.

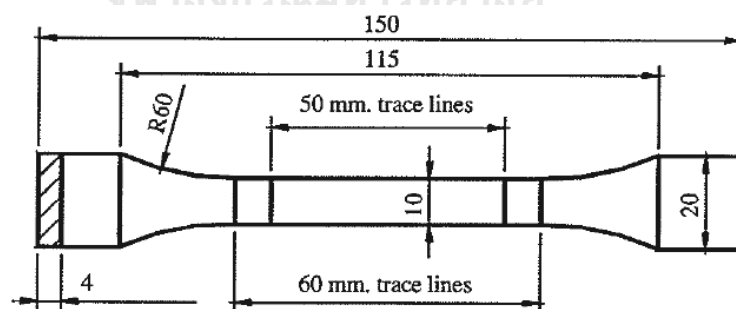


Figure 3.1 Tensile test specimen [32].

3.4.3 Flexural properties

The flexural properties of test specimen were determined according to ISO 178:2010. Flexural properties was measured using universal testing machine (INSTRON, 5967) with cross head speed of 2 mm/min at the test condition of $23 \pm 2^\circ\text{C}$ and $50 \pm 5\% \text{RH}$. An average of five specimens was reported as a representative value. The Flexural specimen is shown in Figure 3.2.

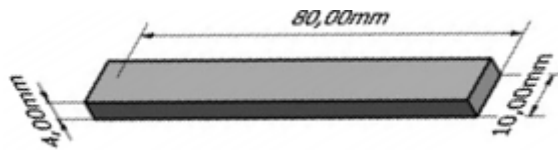


Figure 3.2 Flexural test specimen [33].

3.4.4 Charpy impact strength

The Charpy impact strength of test specimen was determined according to ISO 179-1:2010. Charpy impact strength was measured using Charpy impact machine (Toyo Seiki, DG-CB) at the test condition of $23 \pm 2^\circ\text{C}$ and $-30 \pm 2^\circ\text{C}$. An average of ten specimens was reported as a representative value. The Charpy specimen with notch is shown in Figure 3.3.

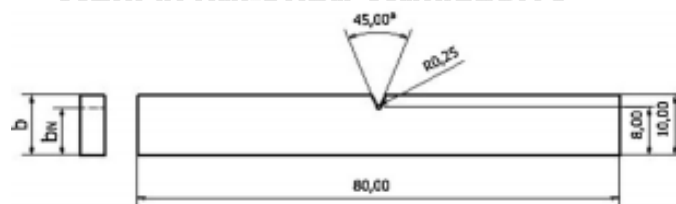


Figure 3.3 Charpy impact strength test specimen [33].

3.4.5 Izod impact strength

The Izod impact strength of test specimen was determined according to ISO 180:2000. Izod impact strength was measured by Izod impact machine (Yasuda, 258-PCS) at the test condition of $23 \pm 2^\circ\text{C}$ and $-30 \pm 2^\circ\text{C}$. An average of eight specimens was reported as a representative value. The Izod specimen with notch is shown in Figure 3.4.

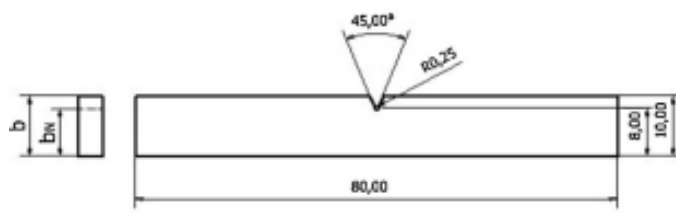


Figure 3.4 Izod impact strength test specimen [33].

3.4.6 Shrinkage

The Shrinkage of test specimen was determined according to ISO 294-4:2001. Shrinkage was measured using profile projector (NIKON, V-12B) at the test condition of $23 \pm 2^\circ\text{C}$ and $50 \pm 5\% \text{RH}$. An average of five specimens was reported as a representative value. The %shrinkage on machine direction (MD) and transverse machine direction (TD) were recorded and determined as an average. The shrinkage specimen is shown in Figure 3.5.

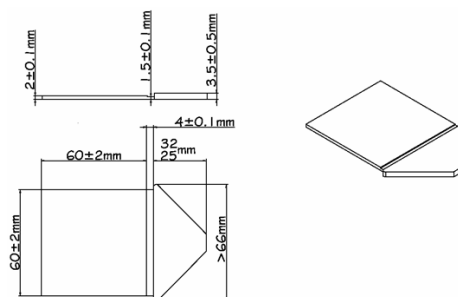


Figure 3.5 shrinkage test specimen [34].

3.4.7 Hardness

The Shore-D hardness of test specimen was determined according to ISO 868:2003. Shore-D hardness was measured using Durometer hardness (Mitutoyo, 811-334-10) at the test condition of $23 \pm 2^\circ\text{C}$ and $50 \pm 5\% \text{RH}$. The thickness of test specimen was at least 6 mm. An average of five specimens was reported as a representative value.

3.4.8 Heat distortion temperature

The heat distortion temperature (HDT) of test specimen was determined according to ISO 75-1:2013. The heat distortion temperature was measured using heat deflection testers (Coesfeld, TESTER-3636) with heating rate 120°C/h. , the outer fiber stress used for testing was 0.45 MPa. An average of three specimens was reported as a representative value. The heat distortion temperature specimen is shown in Figure 3.6.

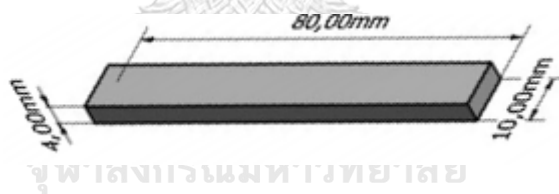


Figure 3.6 heat distortion temperature test specimen [33].

3.4.9 Extraction content by N-decane

The propylene copolymer matrix, wherein the propylene copolymer comprises co-monomer units derived from ethylene and from a C-4 to C-12 alpha-olefin such as 1-butene, 1-hexene or 1-octene content of samples was extracted according to ISO 6427:2013. The extraction content was measured by dissolving the pellet sample in N-decane at 140°C for 1 h and extraction with acetone at the test condition of $23 \pm 2^\circ\text{C}$ and 50-70%RH for 1 h. The extraction content of the PP compounds was determined by Equation (1);

$$\text{Extraction content (\%)} = \frac{\text{Weight of extracted sample}}{\text{Weight of pellet sample}} \times 100 \quad (1)$$

3.4.10 Thermal properties

The T_m , T_c and melting enthalpy of the sample was determined using differential scanning calorimetry (DSC; PerkinElmer) under N_2 atmosphere. The sample was heated from 25°C to 230°C at a rate of $10^\circ\text{C}/\text{min}$ and held isothermally for 5 min to release the melt history. After that, the sample was cooled to 25°C at a rate of $10^\circ\text{C}/\text{min}$ under N_2 atmosphere and then heated to 230°C at the same rate. The degree of crystallinity (X_c) of the PP compounds was calculated using the following Equation (2) [23];

$$\text{Crystallinity, } X_c(\%) = \frac{\Delta H}{\Delta H_M^o} \times 100 \quad (2)$$

where ΔH_M^o and ΔH refer to melting enthalpy for 100% crystalline polypropylene of 209 J/g and melting enthalpy for PP compounds sample, respectively.

3.5 Morphological Investigation มหาวิทยาลัย

The morphology PP compound sample was analyzed by scanning electron microscopy (SEM), (JEOL, JSM-6340LV) with 20 kV acceleration and X3000 magnification. The test specimen was etched in liquid nitrogen as least 3 h, then, immediately broke the specimen using charpy impact tester. After that, all specimens was immersed in N-heptane at ambient temperature for 24 h to remove metallocene elastomer to observe the dispersed phase morphology of elastomer and dried to remove the solvent. Before investigation, specimen was coated with a thin gold layer. The average particle area and aspect ratio of extracted rubber were calculated by Equation (3) and (4) [26], respectively;

$$\text{Average particle area of extracted rubber} = \pi X \left(\frac{L}{2}\right) X \left(\frac{w}{2}\right) \quad (3)$$

$$\text{Aspect ratio of extracted rubber} = \left(\frac{L}{w}\right) \quad (4)$$

where L and W refer to length and width of extracted rubber, respectively.



CHARTER IV

RESULTS AND DISCUSSIONS

4.1 Effect of polypropylene, metallocene elastomer type and blending ratio on physical properties of blends

The physical properties of the PP/POE blends at various types (H-PP/EBR, H-PP/EOR, C-PP/EBR and C-PP/EOR) and blending ratio (100/0, 85/15, 70/30 and 55/45) were investigated to find the appropriate PP and POE type and blending ratios of PP/POE blends for automotive application. The melt flow index, impact properties, tensile properties, flexural properties, shore-d hardness, heat distortion temperature, %shrinkage, %crystallinity and extraction content of the blends are presented in section 4.1.1-4.1.7

4.1.1 Melt flow index

The melt flow index (MFI) measures the flowability of extrusion of blends under specified conditions of temperature and load which is necessary to control the automotive part thickness. The MFI properties of PP/POE blends at various blending ratios are presented in Table 4.1 and Figure 4.1. The MFI of blends decreased with increasing POE (EBR, EOR) content up to 45 wt% (from 69.3-69.6 g/10min for neat PP to 28.0-35.6 g/10min for PP/POE45). This can be explained that the addition of POE increased the entanglement of molecular chains which affected the mobility of molecules [23].

The higher MFI of H-PP/POE blends (35.6-58.4 g/10min) were observed in comparison with C-PP/POE blends (28.0-48.4 g/10min). It implied that the entanglement of C-PP/POE blends was higher than that of H-PP/POE blends due to high co-monomer content (23.0-47.5 wt%) of C-PP/POE blends in consistent with the result of extraction content of blends.

In addition, the MFI of H-PP/EOR blends (38.5-58.4 g/10min) were significantly higher than that of H-PP/EBR blends (35.6-54.5 g/10min). The MFI of

C-PP/EOR blends did not significantly change with increasing EOR content up to 15 wt%. At 30 and 45 wt% of POE, the MFI of C-PP/EOR blends (32.6-34.7 g/10min) were higher than that of C-PP/EBR blends (28.0-33.0 g/10min). This can be explained by the similar behavior of the C-PP/POE blends to H-PP/POE blends as above discussion.

Table 4.1 Effect of PP and POE type and blending ratio on melt flow index of blends

Sample	Melt flow index (g/10min)	Sample	Melt flow index (g/10min)
H-PP	69.6 ± 0.34	C-PP	69.3 ± 0.21
H-PP/EBR15	54.5 ± 0.03	C-PP/EBR15	48.4 ± 0.19
H-PP/EBR30	39.2 ± 0.24	C-PP/EBR30	33.0 ± 0.06
H-PP/EBR45	35.6 ± 0.03	C-PP/EBR45	28.0 ± 0.20
H-PP/EOR15	58.4 ± 0.30	C-PP/EOR15	48.3 ± 0.04
H-PP/EOR30	46.0 ± 0.43	C-PP/EOR30	34.7 ± 0.04
H-PP/EOR45	38.5 ± 0.20	C-PP/EOR45	32.6 ± 0.40

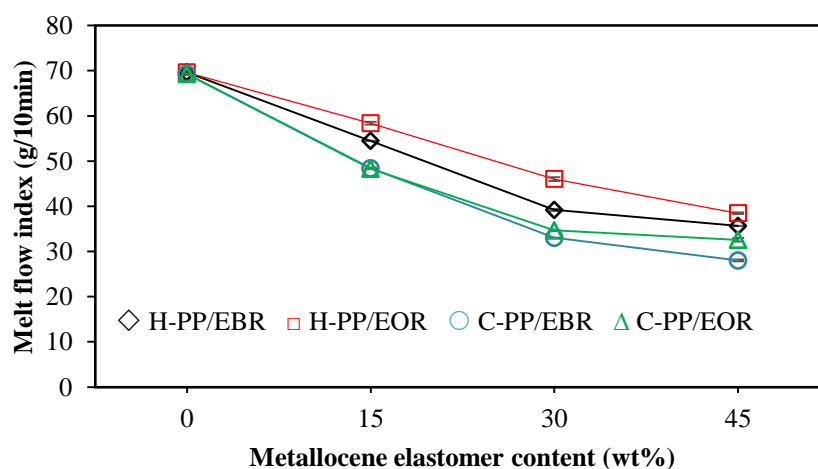


Figure 4.1 Effect of PP and POE type and blending ratio on melt flow index of blends.

The extraction content is one property which has significant influence on the physical properties, especially MFI and impact resistance of blends. The extraction content was the small amounts of undesirable low tacticity and low molar fractions (co-monomer units derived from ethylene and from a C-4 to C-12 alpha-olefin such as 1-butene or 1-octene content) in the PP/POE blend. From Table 4.2 and Figure 4.2, the extraction content of PP/POE blend increased with the presence of POE. The PP/EBR blends had higher extraction content than PP/EOR, since EBR has high co-monomer (17.9 mol% of butene) than EOR (13.6 mol% of octene). As a comparison of H-PP and C-PP, the extraction content of C-PP/POE blends were higher than that of H-PP/POE. These results may be explained by high ethylene content of C-PP (9.4 wt%) than H-PP (0 wt%). However, the extraction content of PP/POE blend (H-PP/EBR, H-PP/EOR, C-PP/EBR and C-PP/EOR) at blending ratio of 55/45 was about the same (46.7-47.5 wt%) due to the limitation of test method. Figure 4.3 shows the relation of extraction content and MFI. The MFI significantly decreased with increasing extraction content.

Table 4.2 Effect of PP and POE type and blending ratio on extraction content of blends

Sample	Extraction content (wt%)	Sample	Extraction content (wt%)
H-PP	0.0	C-PP	9.4
H-PP/EBR15	16.0	C-PP/EBR15	23.0
H-PP/EBR30	32.1	C-PP/EBR30	42.3
H-PP/EBR45	47.2	C-PP/EBR45	47.5
H-PP/EOR15	13.7	C-PP/EOR15	22.9
H-PP/EOR30	27.1	C-PP/EOR30	36.0
H-PP/EOR45	46.7	C-PP/EOR45	47.3

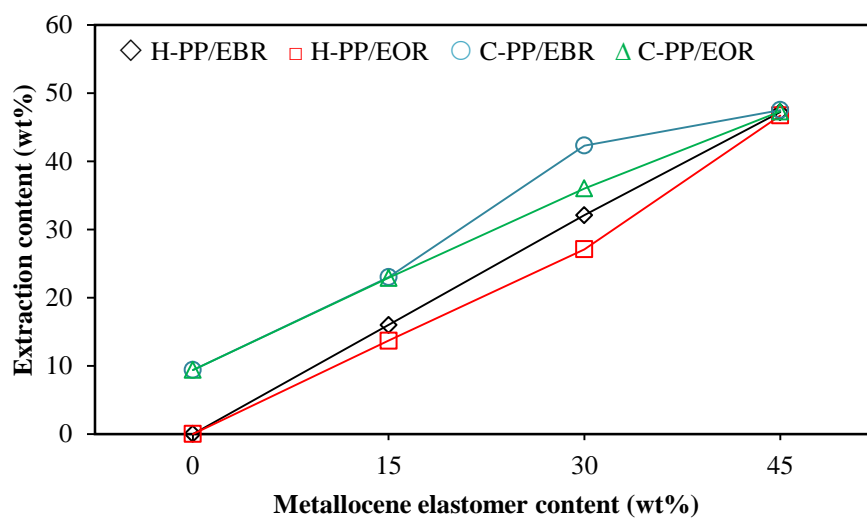


Figure 4.2 Effect of PP and POE type and blending ratio on extraction content of blends.

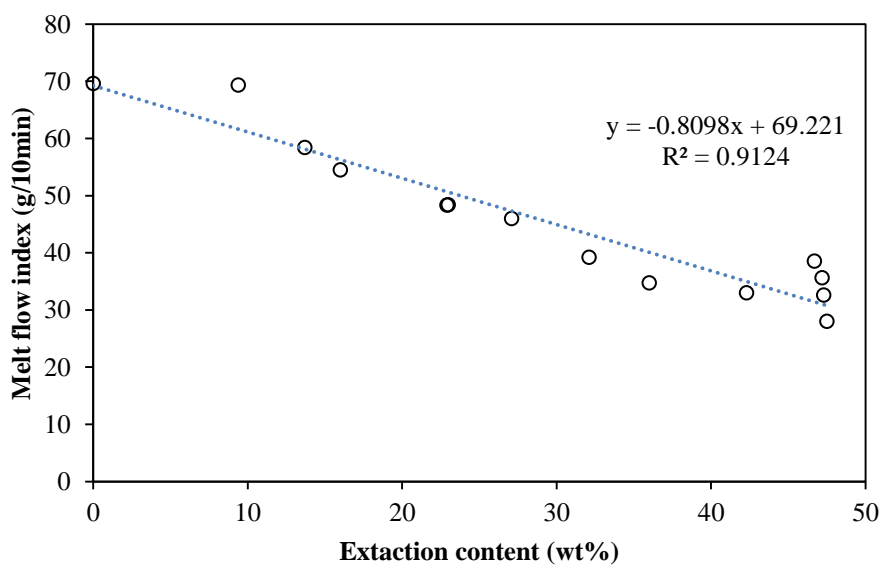


Figure 4.3 The relation between extraction content and melt flow index of blends.

4.1.2 Impact properties

The impact properties determine the amount of energy absorbed by a material during fracture which is widely used in automotive application e.g. bumper. Table 4.3 and Figure 4.4 (a-d) shows the impact properties of PP/POE blends, including Izod and Charpy impact strength at the test condition of 23°C, -30°C.

From Figure 4.4 (a), the charpy impact strength at 23°C of PP/POE blends increased with increasing POE content (from 2.2-6.0 kJ/m² for neat PP to 45.2-68.9 for PP/POE45). The charpy impact strength at 23°C of C-PP/POE blends (10.2-68.9 kJ/m²) was higher than that of H-PP/POE blends (4.4-55.4 kJ/m²) due to high ethylene content of C-PP (9.4 wt%) than H-PP (0 wt%). The charpy impact strength at 23°C of C-PP/POE blends rapidly increased when the POE was higher than 15 wt% (from 10.2-10.8 kJ/m² for C-PP/POE15 to 47.8-53.3 kJ/m² for C-PP/POE30) while, the charpy impact strength at 23°C of H-PP/POE blends was significantly changed at the POE content above 30 wt% (from 9.0-16.1 kJ/m² for H-PP/POE30 to 45.2-55.4 kJ/m² for H-PP/POE45). In addition, the charpy impact strength at 23°C of PP/EOR blends (5.1-68.9 kJ/m²) was higher than that of PP/EBR (4.4-52.5 kJ/m²). This phenomenon can be explained that the higher molecular weight or the longer side chain of EOR than EBR resulting the high entanglement in blends [30].

From Figure 4.4 (b), the izod impact strength at 23°C of PP/POE blends increased with increasing POE content (from 3.9-5.3 kJ/m² for neat PP to 34.7-52.7 kJ/m² for PP/POE45) blends which is similar to Figure 4.4 (a). The izod impact strength at 23°C of C-PP/POE blends (10.3-52.7 wt%) was higher than H-PP/POE blends (5.2-44.3 wt%). In addition, the izod impact strength at 23°C of C-PP/POE and H-PP/POE blends rapidly increased when the POE was higher than 15 wt% (from 10.3-10.7 kJ/m² for C-PP/POE15 to 42.2-48.9 kJ/m² for C-PP/POE30 and from 5.2-5.3 kJ/m² for H-PP/POE15 to 18.3-20.5 kJ/m² for H-PP/POE30), this behavior similar to Figure 4.4 (a). Furthermore, the izod impact strength at 23°C of dispersed EOR in blends (5.3-52.7 wt%) was higher than EBR (5.2-45.6 kJ/m²). This can be explained by the similar behavior of the charpy impact strength at 23°C of PP/POE blends as above discussion (Figure 4.4, a).

From Figure 4.4 (c), the charpy impact strength at -30°C of PP/POE blends increased with increasing POE content (from 1.1-2.3 kJ/m² for neat PP to 10.0-

73.1 kJ/m² for PP/POE45) blends. The charpy impact strength at -30°C of C-PP/POE blends (4.9-73.1 wt%) was higher than that of H-PP/POE blends (1.2-10.0 wt%). The charpy impact strength at -30°C of C-PP/POE and H-PP/POE blends was significantly improved at POE content above 30 wt% (from 6.4-8.4 kJ/m² for C-PP/POE30 to 61.7-73.1 kJ/m² for C-PP/POE45 and from 2.0-2.7 kJ/m² for H-PP/POE30 to 7.4-10.0 kJ/m² for H-PP/POE45). However, the dispersed EOR and EBR in PP/POE blends did not significantly affect the charpy impact strength at -30°C except, C-PP/EBR45 blend (73.1 kJ/m²) had higher than C-PP/EOR45 blend (61.7 kJ/m²) due to the agglomeration of EBR. This phenomenon can be explained that the higher molecular weight or the longer side chain of EOR than EBR resulting high entanglement in blends [30].

From Figure 4.4 (d), the izod impact strength at -30°C of PP/POE blends increased with increasing POE content (from 1.3-3.7 kJ/m² for neat PP to 11.2-61.7 kJ/m² for PP/POE45) blends. The izod impact strength at -30°C of C-PP/POE blends (5.6-61.7 wt%) was higher than that of H-PP/POE blends (1.3-11.2 wt%). In addition, the izod impact strength at -30°C of C-PP/POE and H-PP/POE blends rapidly increased when the POE was higher than 30 wt% which is similar to Figure 4.4 (c) (from 7.3-8.1 kJ/m² for C-PP/POE30 to 60.5-61.7 kJ/m² for C-PP/POE45 and from 2.8-3.5 kJ/m² for H-PP/POE30 to 9.2-11.2 kJ/m² for H-PP/POE45). However, the dispersed EOR and EBR in PP/POE blends did not show the significant difference on izod impact strength at -30°C. This can be explained by the similar behavior of the charpy impact strength at 23°C of PP/POE blends as above discussion (Figure 4.4 (c)).

POE had a good compatibility with PP matrix, so POE should act as the center of the stress concentration to induce a large of the crazes and shear bands. At the same time, an important factor for impact improvement is rubber particle size and dispersion. So, the morphological properties of blends were also investigated in section 4.2 to obtain the relation of material performance and the morphology.

Table 4.3 Effect of PP and POE type and blending ratio on impact properties of blends

Sample	Charpy impact	Charpy impact	Izod impact	Izod impact
	strength at 23°C (kJ/m ²)	strength at -30°C (kJ/m ²)	strength at 23°C (kJ/m ²)	strength at -30°C (kJ/m ²)
H-PP	2.2 ± 0.34	1.1 ± 0.03	3.9 ± 0.82	1.3 ± 0.13
H-PP/EBR15	4.4 ± 0.91	1.2 ± 0.19	5.2 ± 1.34	1.3 ± 0.41
H-PP/EBR30	9.0 ± 0.58	2.1 ± 0.09	18.3 ± 2.59	2.8 ± 0.09
H-PP/EBR45	45.2 ± 2.17	10.0 ± 0.75	34.7 ± 3.14	11.2 ± 1.08
H-PP/EOR15	5.1 ± 0.35	1.2 ± 0.21	5.3 ± 0.43	1.4 ± 0.16
H-PP/EOR30	16.1 ± 0.77	2.7 ± 0.43	20.5 ± 2.29	3.5 ± 0.09
H-PP/EOR45	55.4 ± 1.43	7.4 ± 0.64	44.3 ± 1.16	9.2 ± 1.10
C-PP	6.0 ± 0.16	2.3 ± 0.06	5.3 ± 0.30	3.7 ± 0.15
C-PP/EBR15	10.2 ± 0.51	4.9 ± 0.12	10.3 ± 0.27	5.6 ± 0.34
C-PP/EBR30	47.8 ± 0.51	8.4 ± 0.25	42.2 ± 0.25	8.1 ± 0.21
C-PP/EBR45	52.5 ± 2.62	73.1 ± 0.90	45.6 ± 1.36	60.5 ± 0.87
C-PP/EOR15	10.8 ± 0.49	4.5 ± 0.16	10.7 ± 0.63	5.5 ± 0.48
C-PP/EOR30	53.3 ± 0.70	6.4 ± 0.17	48.9 ± 0.88	7.3 ± 0.22
C-PP/EOR45	68.9 ± 0.93	61.7 ± 1.84	52.7 ± 0.72	61.7 ± 0.91

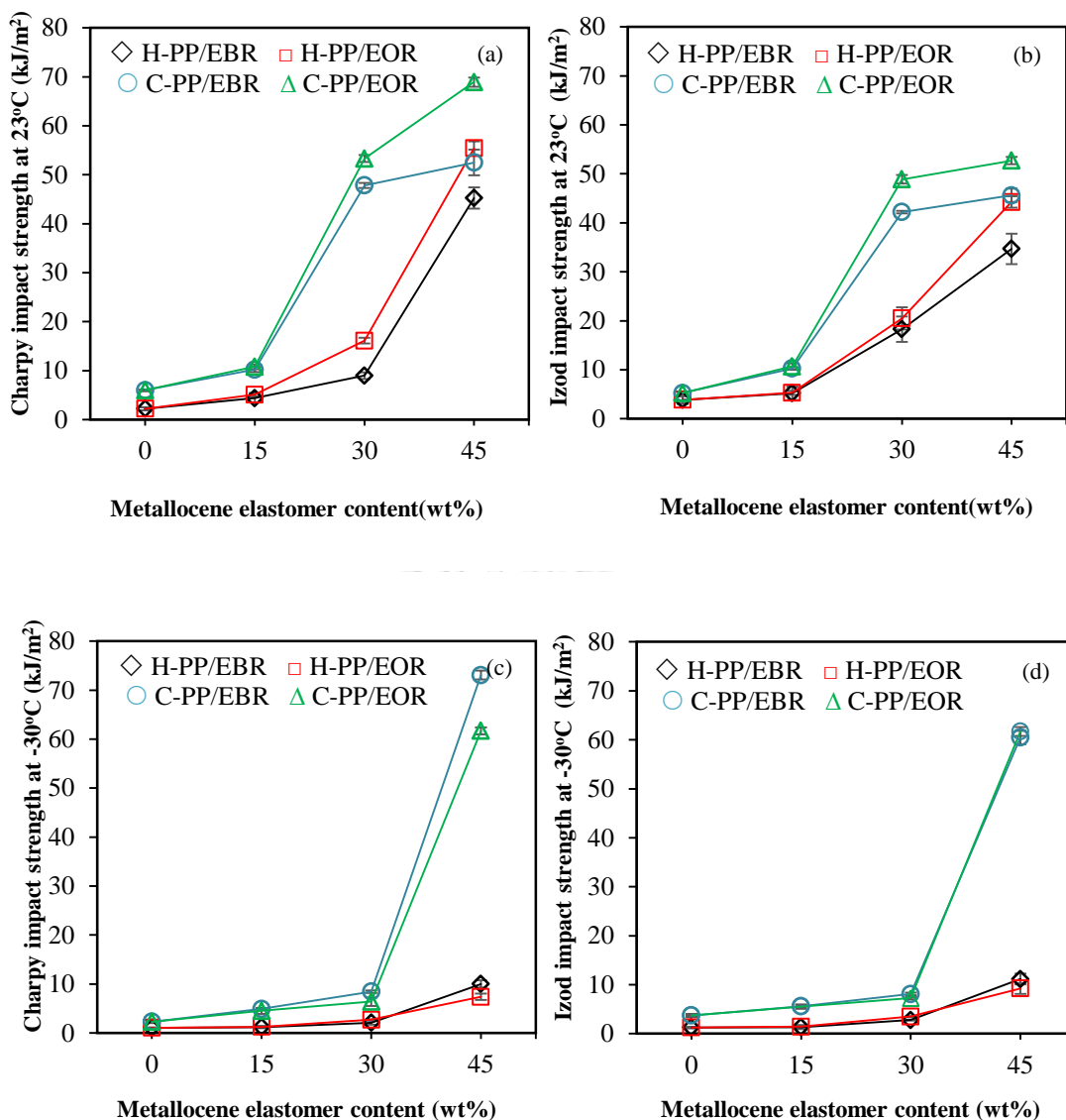


Figure 4.4 Effect of PP and POE type and blending ratio on impact properties of blends; (a) Charpy impact strength at 23°C, (b) Izod impact strength at 23°C, (c) Charpy impact strength at -30°C, (d) Izod impact strength at -30°C.

4.1.3 Tensile properties

The tensile properties measure the resistance of PP/POE blends to a static or slowly applied force. The tensile strength, elongation at break and tensile modulus of blends at 23°C are presented in Table 4.4 and Figure 4.5 (a-c).

From Figure 4.5 (a), the tensile strength of blends decreased with increasing POE content up to 45 wt% (from 31.2-36.8 MPa for neat PP to 12.0-16.2 MPa for PP/POE45). This could be due to the elastomeric nature of POE. The strength of elastomer was lower than that of PP matrix [36]. The tensile strength of H-PP/POE blends (13.0-28.0 MPa) was higher than that of C-PP/POE blends (12.0-23.8 MPa). In addition, the tensile strength of PP/EOR blends (13.9-28.0 MPa) was higher than that of PP/EBR blends (12.0-27.3 MPa). This can be explained that the crystallinity of EOR (19%) was higher than that of EBR (13%) [35].

From Figure 4.5 (b), the elongation at break of PP/POE blends was improved with increasing the POE content (from 27% for neat PP to 500% for PP/POE45). This can be explained that the elastomeric nature of POE performed as stress concentrator in the tensile testing, and stress concentrator could lead to yielding and crazing around the PP matrix. So the elastomeric can absorb high energy to avoid a highly strain process [35]. The elongation at break of the H-PP/POE blends was significantly increased when adding the POE content at 15 wt% (from 35.2 for H-PP to >500% for H-PP/POE15) while the elongation at break of C-PP/POE was slightly increased (from 27.4 for C-PP to 44.8-65.6% for C-PP/POE15). These results can be explained that the existence of more finely dispersed POE in the H-PP matrix (Figure 4.11) than that of C-PP/POE blends (Figure 4.12) significantly contribute to the improved toughness behavior, either by crazing or by shear-yielding deformation mechanisms. The partial incorporation of POE molecules in the intercrystalline regions of PP spherulites and also in the amorphous regions enable a more effective stress transfer between the materials, allowing H-PP a higher deformation and an enhanced toughness behavior [36]. However, there is no significant difference on elongation at break of dispersed EOR and EBR in PP/POE blends except, C-PP/EOR30 (>500%) had higher elongation at break than C-PP/EBR30 blends (110%).

From Figure 4.5 (c), the tensile modulus of PP/POE blends decreased significantly due to the presence of POE. When the content of POE was 45 wt%, the

tensile modulus of PP/POE blends decreased from 1709.4-1714.7 MPa to 599.4-621.6 MPa. This phenomenon is similar to Figure 4.5 (a). However, there is no significant difference on the tensile modulus of PP/POE blends when the PP matrix (H-PP and C-PP) and POE type (EBR and EOR) were changed.

Table 4.4 Effect of PP and POE type and blending ratio on tensile properties of blends

Sample	Tensile strength (MPa)	Elongation at break (%)	Tensile modulus (MPa)
H-PP	36.8 ± 0.10	35.2 ± 5.01	1709.4 ± 38.1
H-PP/EBR15	27.3 ± 0.67	> 500 ± 7.38	1359.5 ± 52.9
H-PP/EBR30	18.9 ± 0.15	> 500 ± 1.34	1034.8 ± 27.5
H-PP/EBR45	13.4 ± 0.16	> 500 ± 2.94	599.4 ± 34.4
H-PP/EOR15	28.0 ± 0.11	> 500 ± 0.21	1318.5 ± 30.7
H-PP/EOR30	21.4 ± 0.18	> 500 ± 2.11	1074.7 ± 19.8
H-PP/EOR45	16.2 ± 0.19	> 500 ± 2.15	782.9 ± 11.5
C-PP	31.2 ± 0.12	27.4 ± 1.13	1714.7 ± 34.4
C-PP/EBR15	22.8 ± 0.06	44.8 ± 2.75	1288.2 ± 34.0
C-PP/EBR30	16.6 ± 0.11	110 ± 13.8	942.1 ± 29.9
C-PP/EBR45	12.0 ± 0.19	475 ± 7.69	621.6 ± 24.8
C-PP/EOR15	23.8 ± 0.05	65.6 ± 1.48	1313.5 ± 35.7
C-PP/EOR30	17.7 ± 0.06	> 500 ± 35.3	940.2 ± 26.1
C-PP/EOR45	13.9 ± 0.06	461 ± 18.2	725.8 ± 22.3

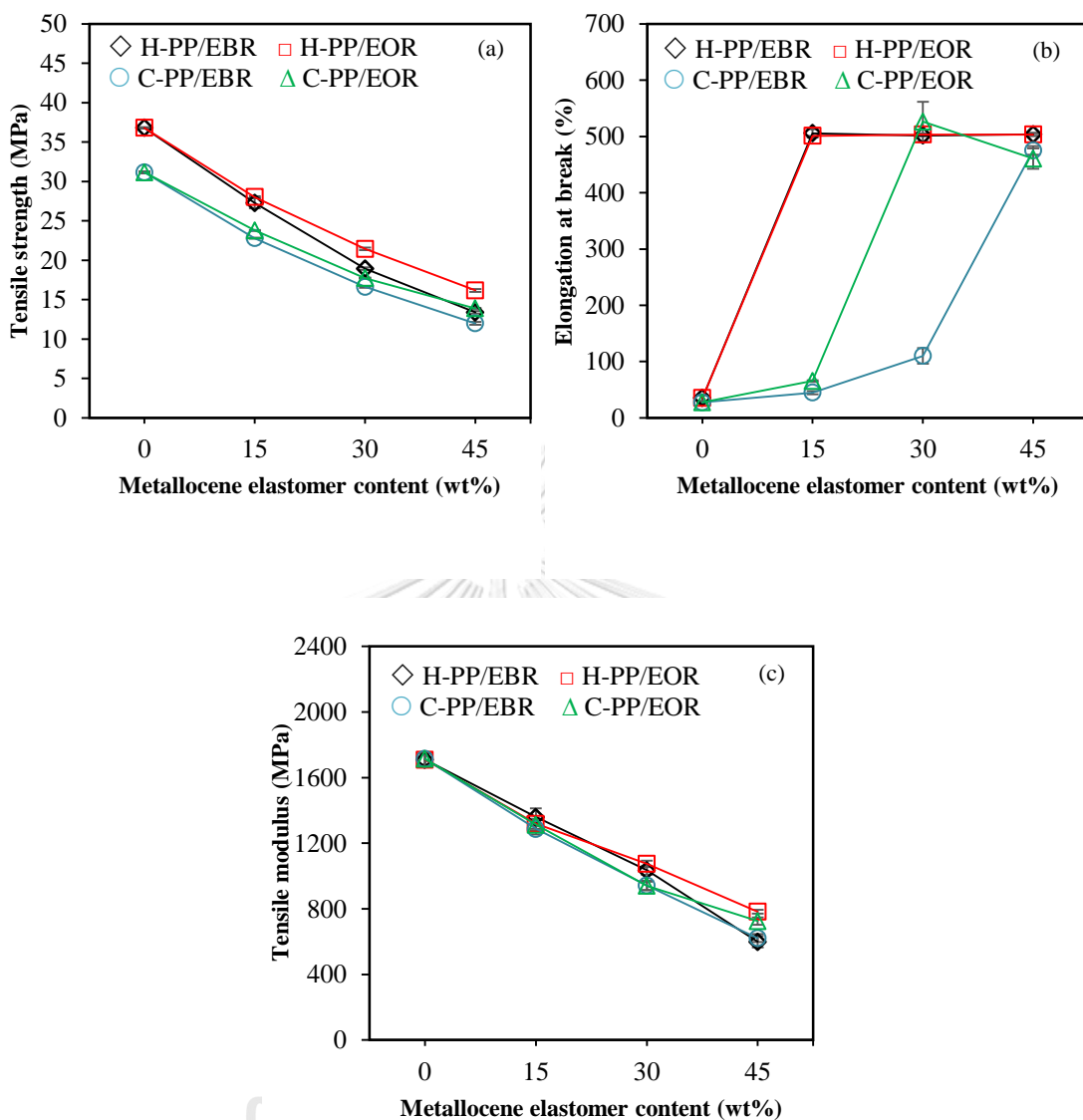


Figure 4.5 Effect of PP and POE type and blending ratio on tensile properties of blends; (a) Tensile strength, (b) % Elongation at break, (c) Tensile modulus.

4.1.4 Flexural properties

The flexural properties at 23°C of PP/POE blends are considered as an essential requirement for the automotive parts. The effect of PP and POE type and blending ratio are presented in Tale 4.5 and Figure 4.6.

From Figure 4.6 (a), the flexural strength of PP/POE blends decreased with increasing the POE content (from 43.3-45.2 MPa for neat PP to 13.9-15.4 MPa for PP/POE45). This can be explained that the addition of POE decreased the crystallinity of blends (from 46.6-48.8% for neat PP to 10.3-21.2 for PP/POE45) [35]. The flexural strength of H-PP/POE blends (15.4-33.8 MPa) was higher than that of C-PP/POE blends (13.9-31.9 MPa). In addition, the flexural strength of H-PP/EBR (15.4-33.0 MPa) and C-PP/EBR (13.9-31.2 MPa) was lower than that of H-PP/EOR (18.3-33.8 MPa) and C-PP/EOR (15.9-31.9 MPa), respectively, due to that the crystallinity of EOR (19%) was higher than that of EBR (13%).

From Figure 4.6 (b), the flexural modulus of PP/POE blends decreased with increasing POE content (from 1680.9-1741.8 MPa for neat PP to 573.7-615.7 MPa for PP/POE45). The flexural modulus of H-PP/POE (615.7-1316.9 MPa) was higher than that of C-PP/POE blends (573.7-1318.4 MPa). In addition, the flexural modulus of H-PP/EBR (615.7-1316.9 MPa) and C-PP/EBR (573.7-1289.0 MPa) were lower than that of H-PP/EOR (741.4-1263.1 MPa) and C-PP/EOR (681.6-1318.4 MPa), respectively. This can be explained by the similar behavior to the flexural strength of PP/POE blends as above discussion (Figure 4.6, a).

Table 4.5 Effect of PP and POE type and blending ratio on flexural properties of blends

Sample	Flexural Strength (MPa)	Flexural Modulus (MPa)	Sample	Flexural Strength (MPa)	Flexural Modulus (MPa)
H-PP	45.2 ± 0.32	1741.8 ± 87.2	C-PP	43.3 ± 0.44	1680.9 ± 52.2
H-PP/EBR15	33.0 ± 0.80	1316.9 ± 13.3	C-PP/EBR15	31.2 ± 0.28	1289.0 ± 47.7
H-PP/EBR30	23.0 ± 0.30	1013.3 ± 18.2	C-PP/EBR30	21.2 ± 0.19	892.3 ± 15.4
H-PP/EBR45	15.4 ± 0.12	615.7 ± 23.3	C-PP/EBR45	13.9 ± 0.18	573.7 ± 17.5
H-PP/EOR15	33.8 ± 0.08	1263.1 ± 41.7	C-PP/EOR15	31.9 ± 0.24	1318.4 ± 50.1
H-PP/EOR30	25.8 ± 0.17	1051.1 ± 44.3	C-PP/EOR30	22.7 ± 0.08	904.2 ± 37.6
H-PP/EOR45	18.3 ± 0.34	741.4 ± 18.9	C-PP/EOR45	15.9 ± 0.07	681.6 ± 23.2

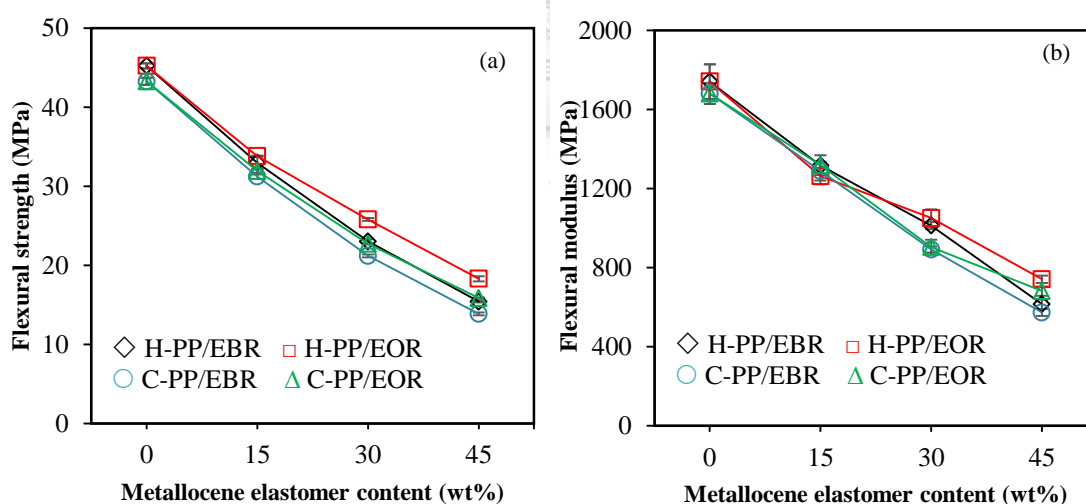


Figure 4.6 Effect of PP and POE type and blending ratio on flexural properties of blends; (a) Flexural strength, (b) Flexural modulus.

4.1.5 Shore-D hardness

Shore-d hardness is measured in term of plastic resistance on surface indentation under specific condition. Shore-D as the preferred method for rubbers or elastomers is also used for soft plastics such as poly-olefins and PP/POE blends. From Table 4.6 and Figure 4.7, the shore-d hardness of blends decreased with increasing POE content (from 68.8-68.9 for neat PP to 48.6-50.5 for PP/POE45), which could be attributed to the low crystallinity of PP/POE blends. Comparison of adding EBR and EOR in the blends, the shore-d hardness did not exhibit the significant difference except at 45wt% of POE content in PP/POE blends. At 45 wt% of POE content, shore-d hardness of H-PP/EOR (53.0) and H-PP/EBR (50.5) were higher than that of C-PP/EOR (50.2) and C-PP/EBR (48.6), respectively. For blends at POE content 0-30 wt%, there is no significant difference on shore-d hardness when the PP matrix (H-PP and C-PP) was changed.

Table 4.6 Effect of PP and POE type and blending ratio on shore-d hardness of blends

Sample	Hardness (Shore D)	Sample	Hardness (Shore D)
H-PP	68.8 ± 0.49	C-PP	68.9 ± 0.42
H-PP/EBR15	64.8 ± 1.20	C-PP/EBR15	62.6 ± 0.86
H-PP/EBR30	57.6 ± 0.40	C-PP/EBR30	57.9 ± 0.55
H-PP/EBR45	50.5 ± 0.37	C-PP/EBR45	48.6 ± 0.42
H-PP/EOR15	64.2 ± 0.83	C-PP/EOR15	63.3 ± 0.38
H-PP/EOR30	58.4 ± 0.19	C-PP/EOR30	58.4 ± 0.48
H-PP/EOR45	53.0 ± 0.96	C-PP/EOR45	50.2 ± 0.31

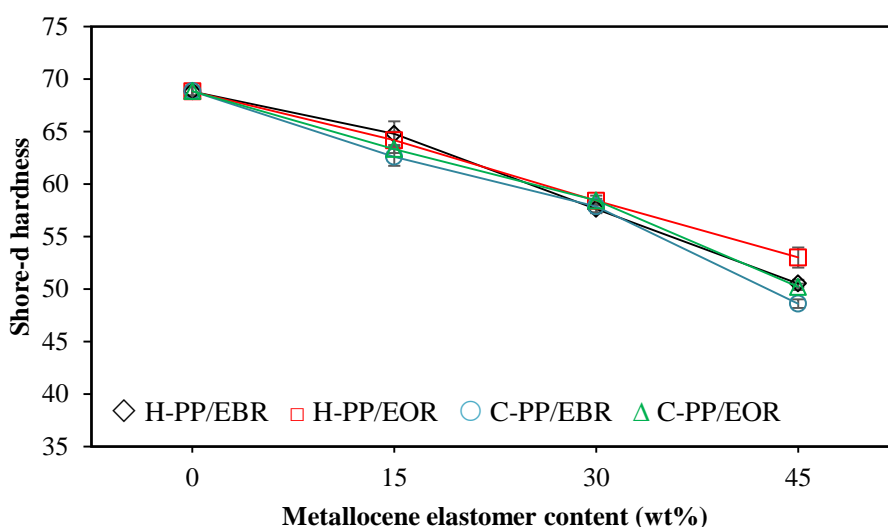


Figure 4.7 Effect of PP and POE type and blending ratio on shore-d hardness of blends.

4.1.6 Heat distortion temperature

Heat distortion temperature (HDT) indicates the temperature that materials start to soften when disclosed to fixed load (0.45 MPa). From Table 4.7 and Figure 4.8, the HDT of PP/POE blends decreased with increasing POE content (from 109.1-109.8 for neat PP to 63.2-65.9 for PP/POE45). This can be explained that the adding POE decreased the crystallinity of the blends [35]. For blends at POE content of 0-30 wt%, the heat distortion temperature of PP/POE blends did not exhibit the significant difference when the PP matrix (H-PP and C-PP) and POE type (EBR and EOR) were changed.

Table 4.7 Effect of PP and POE type and blending ratio on heat distortion temperature of blends

Sample	Heat distortion temperature at 0.45 MPa (°C)	Sample	Heat distortion temperature at 0.45 MPa (°C)
H-PP	109.1 ± 4.71	C-PP	109.8 ± 1.85
H-PP/EBR15	99.1 ± 8.07	C-PP/EBR15	97.3 ± 0.95
H-PP/EBR30	83.2 ± 1.22	C-PP/EBR30	80.8 ± 2.66
H-PP/EBR45	63.2 ± 4.80	C-PP/EBR45	66.3 ± 4.93
H-PP/EOR15	98.1 ± 3.20	C-PP/EOR15	96.3 ± 0.32
H-PP/EOR30	83.8 ± 4.48	C-PP/EOR30	81.2 ± 1.06
H-PP/EOR45	70.6 ± 3.08	C-PP/EOR45	65.9 ± 5.26

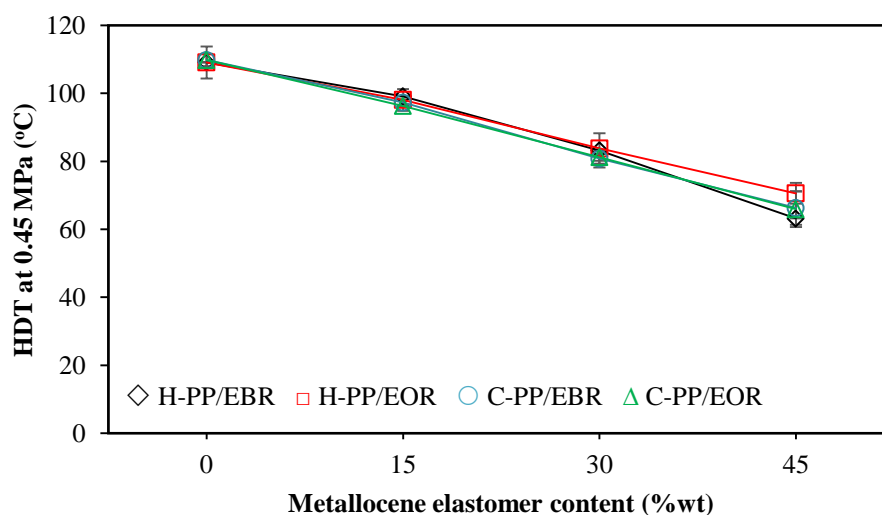


Figure 4.8 Effect of PP and POE type and blending ratio on heat distortion temperature of blends.

4.1.7 Melting temperature (T_m), crystallization temperature (T_c) and %crystallinity (X_c)

Table 4.8 and Figure 4.9 show the melting temperature (T_m), crystallization temperature (T_c), the melting enthalpy (ΔH) and %crystallinity (X_c) of PP/POE blends. The X_c of PP/POE blends decreased with increasing POE content (from 46.6-48.1 % for neat PP to 10.3-21.2% of PP/POE45). For H-PP/EBR, H-PP/EOR, C-PP/EBR and C-PP/EOR blend, the T_m and T_c did not change with increasing POE content. This indicated that the coalescence of POE did not influence the T_m and T_c of PP/POE blends [35]. For comparison of EBR and EOR in H-PP/POE blends, the % crystallinity of H-PP/EOR (23.4-33.3%) was higher than that of the H-PP/EBR blends (21.2-32.7%), it implied that the EOR was an effective nucleating agent in PP matrix. This phenomenon can be explained by the PP molecular chains aggregating to the long EOR molecular chains and crystallizing [37].

Furthermore, the %crystallinity of H-PP/POE blends was lower than C-PP/POE blends at 0-30 wt% of the POE content because the higher crystallinity of neat C-PP (48.1%) than H-PP (46.6%) was observed. Conversely, the %crystallinity of H-PP/POE45 blends (21.2-23.4%) was higher than that of C-PP/POE45 blends (10.3-16.0%). The %crystallinity reflects the total interfaces between crystalline and amorphous material. This means that PP has more total interfaces between crystalline and amorphous material than its blends. Thus, C-PP/POE blends (with co-monomer) has low total interfaces between crystalline and amorphous phase at higher content of POE than 30 wt% [37]. Thus, the %crystallinity was related to the morphological properties of PP/POE blends.

Table 4.8 Effect of PP, POE type and blending ratio on thermal properties of blends

Sample	T _m (°C)	T _c (°C)	ΔH (J/g)	Crystallinity (%)
H-PP	157.9	127.8	96.5	46.6
H-PP/EBR15	157.6	127.8	67.8	32.7
H-PP/EBR30	157.6	127.5	53.5	25.9
H-PP/EBR45	157.7	127.1	43.9	21.2
H-PP/EOR15	157.6	127.8	69.0	33.3
H-PP/EOR30	157.7	127.9	60.8	29.4
H-PP/EOR45	157.8	127.5	48.4	23.4
C-PP	164.5	127.0	99.5	48.1
C-PP/EBR15	164.3	126.3	80.3	38.8
C-PP/EBR30	164.4	126.6	67.4	32.5
C-PP/EBR45	164.4	126.1	21.3	10.3
C-PP/EOR15	164.2	126.8	85.1	41.1
C-PP/EOR30	164.3	126.7	71.6	34.6
C-PP/EOR45	164.2	126.3	33.1	16.0

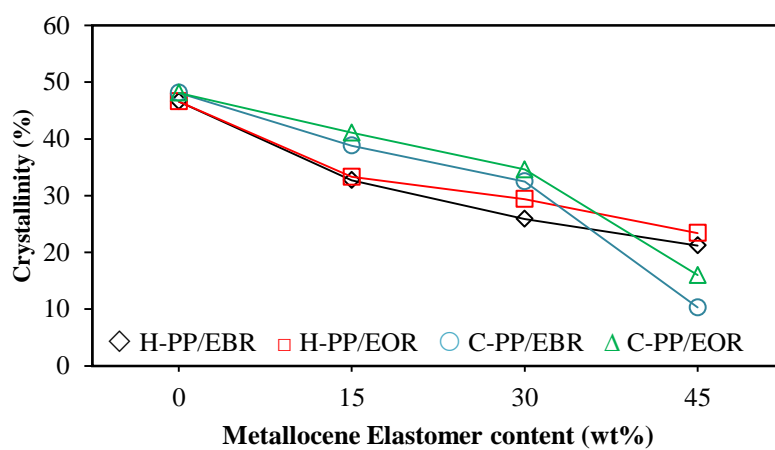


Figure 4.9 Effect of PP and POE type and blending ratio on %crystallinity of blends.

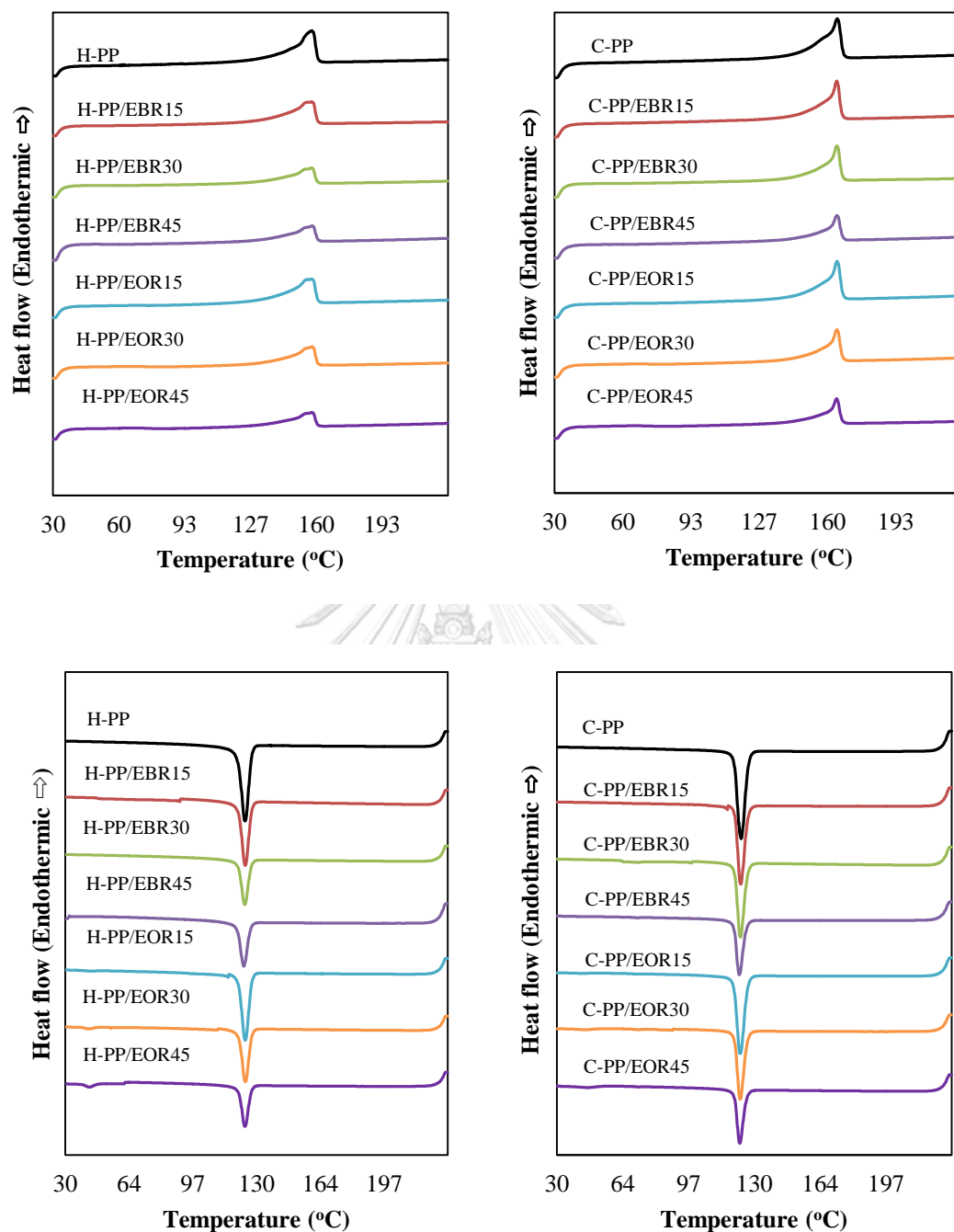


Figure 4.10 DSC thermograms of the PP/POE blends; (a) H-PP/POE blend from the second heating scan, (b) C-PP/POE from the second heating scan, (c) C-PP/POE blend from the cooling scan, (d) C-PP/POE blend from the cooling scan.

4.2 Effect of polypropylene, metallocene elastomer type and blending ratio on morphological properties of blends

The morphology of the impact fracture surface of PP/POE blends (H-PP/EBR, H-PP/EOR, C-PP/EBR and C-PP/EOR) at various blending ratios (100/0, 85/15, 70/30 and 55/45 wt%) is shown in Figure 4.11 and 4.12. For the morphology of homopolymer (H-PP) and copolymer PP (C-PP) (Figure 4.11 (a) and 4.12 (a)), number of holes in the C-PP was observed compared with smooth surface of H-PP (without holes) because C-PP has the ethylene co-monomer dispersed in the PP matrix confirmed by the extraction content (section 4.1.1)

Normally, the dispersion and particle size of POE in the polymer matrix are the main factors to control the physical properties of blends [37]. From Figure 4.11 and Figure 4.12, the minor POE phase was well dispersed in the PP matrix for both H-PP and C-PP blends. In addition, an average particle area of extracted rubber of blends increased with increasing POE content (15-30 wt%). In contrast, the dispersed EBR and EOR elongated in continuous phase (H-PP, C-PP) at 45 wt% of POE were shown in Figure 4.11 (f-g) and Figure 4.12 (f-g).

For the effect of POE type on morphological properties of blends, both blends (PP/EBR, PP/EOR) clearly showed the phase-separated structures, reflecting the immiscibility of the blends [37], where the main matrix is the PP phase and the holes are the extracted rubber phase. At the POE content of 15-30 wt%, no sharply defined interfaces between different domains was observed indicating the good miscibility of the PP/EBR and PP/EOR blends. In addition, an average particle area of extracted rubber of H-PP/EOC blends was lower than that of H-PP/EBR blends [38]. The observed morphological behavior was consistent to the decreased impact properties (section 4.1.2) with increasing an average particle area of the blends. This implied that the small particle area as small particle size affected the improved impact properties [30].

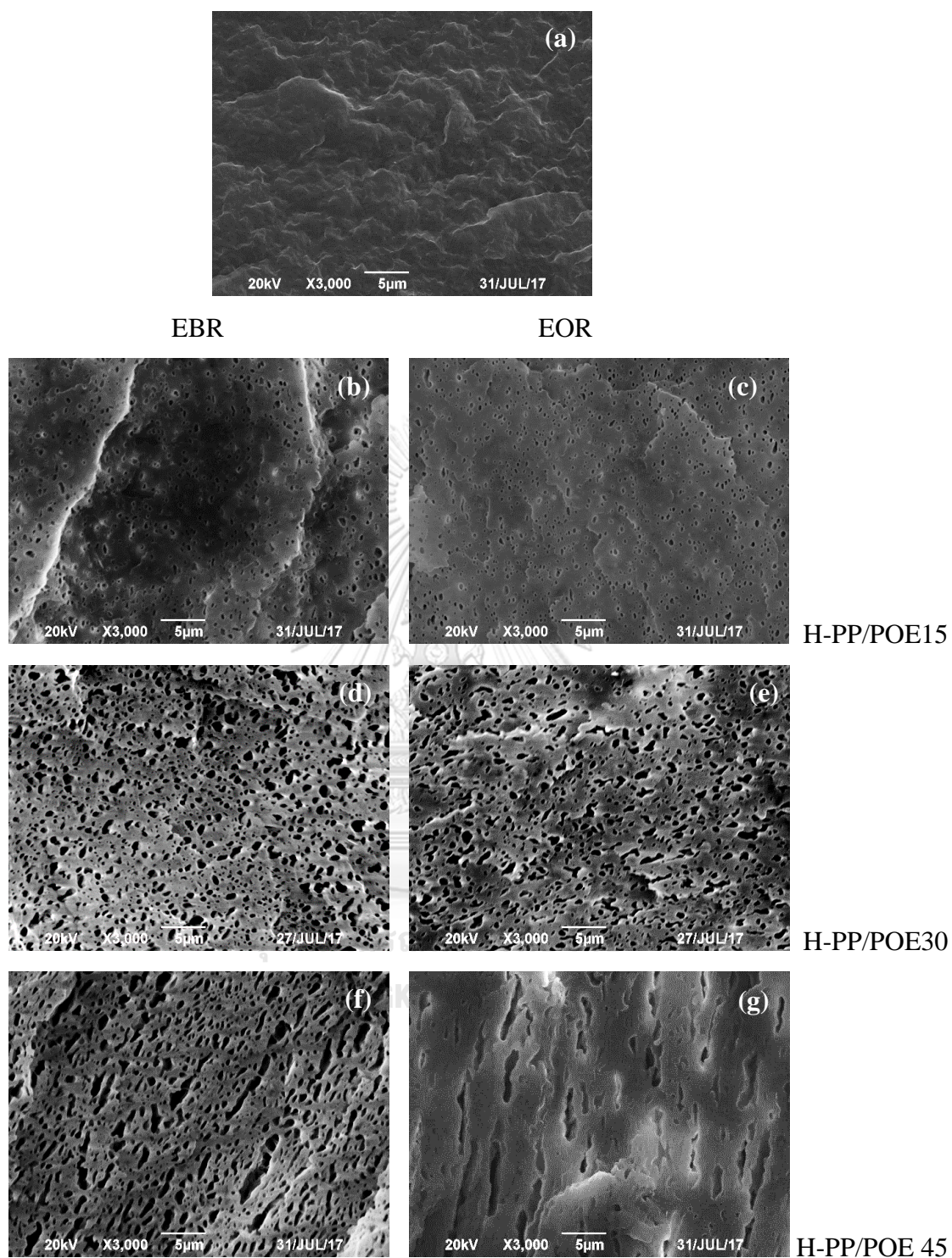


Figure 4.11 SEM micrographs of H-PP/POE blends; (a) H-PP, (b) H-PP/EBR15, (c) H-PP/EOR15, (d) H-PP/EBR30, (e) H-PP/EOR30, (f) H-PP/EBR45, (g) H-PP/EOR45.

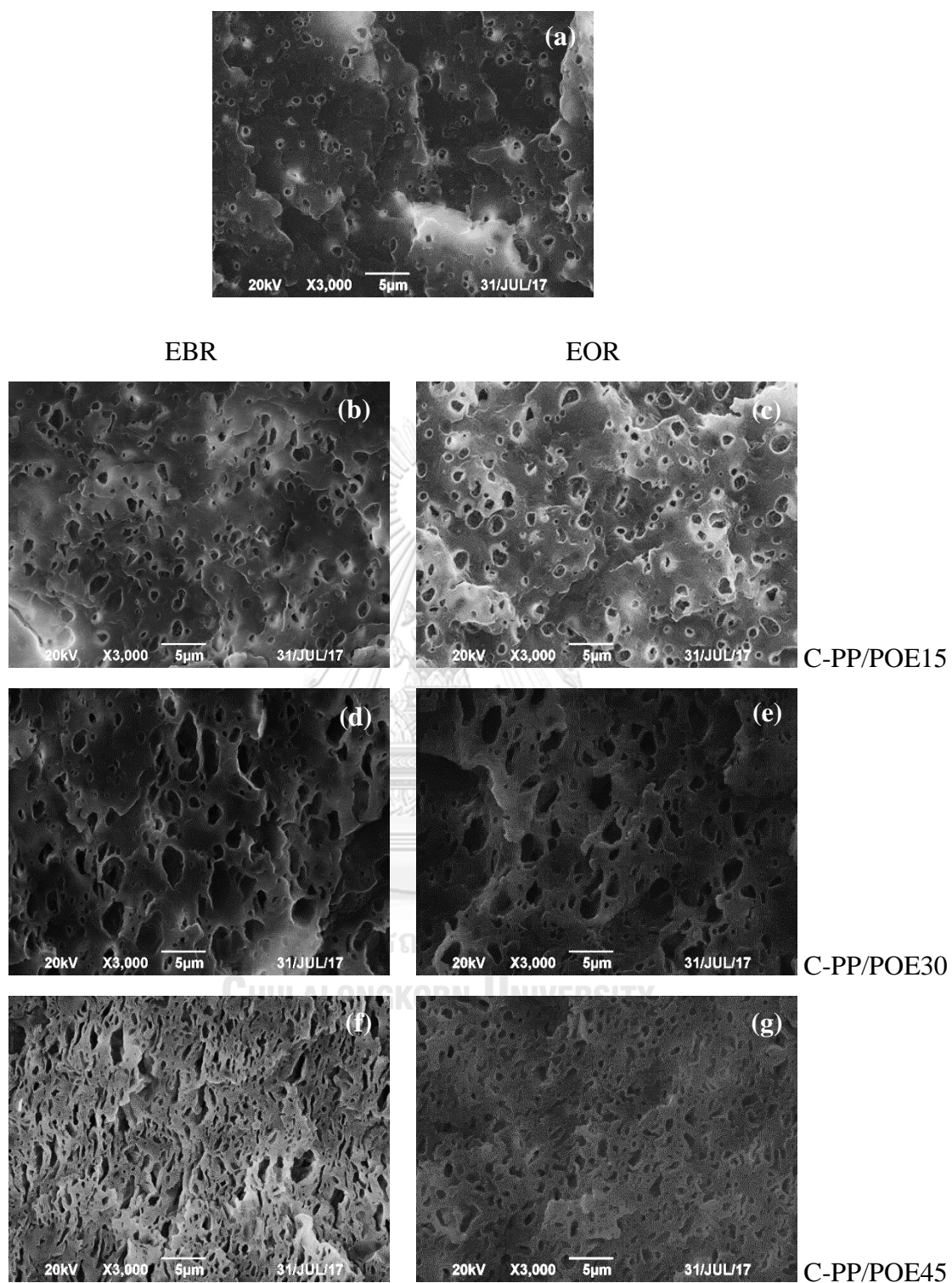


Figure 4.12 SEM micrographs of H-PP/POE blends; (a) H-PP, (b) H-PP/EBR15, (c) H-PP/EOR15, (d) H-PP/EBR30, (e) H-PP/EOR30, (f) H-PP/EBR45, (g) H-PP/EOR45.

Table 4.9 Average particle area of extracted rubber of blends

Sample	Average particle area of extracted rubber (μm^2)	Sample	Average particle area of extracted rubber (μm^2)
H-PP	-	C-PP	0.229 ± 0.082
H-PP/EBR15	0.199 ± 0.085	C-PP/EBR15	0.580 ± 0.203
H-PP/EBR30	0.490 ± 0.089	C-PP/EBR30	2.620 ± 1.706
H-PP/EBR45	0.870 ± 0.746	C-PP/EBR45	1.542 ± 0.842
H-PP/EOR15	0.111 ± 0.042	C-PP/EOR15	0.916 ± 0.308
H-PP/EOR30	0.369 ± 0.095	C-PP/EOR30	2.825 ± 1.594
H-PP/EOR45	7.978 ± 4.857	C-PP/EOR45	1.324 ± 0.784

Table 4.10 Average aspect ratio of extracted rubber of blends

Sample	Aspect ratio of extracted rubber	Sample	Aspect ratio of extracted rubber
H-PP	-	C-PP	1.432 ± 0.357
H-PP/EBR15	1.645 ± 0.481	C-PP/EBR15	1.784 ± 0.598
H-PP/EBR30	1.884 ± 0.731	C-PP/EBR30	2.278 ± 0.789
H-PP/EBR45	2.356 ± 0.928	C-PP/EBR45	3.228 ± 1.051
H-PP/EOR15	1.629 ± 0.355	C-PP/EOR15	1.348 ± 0.343
H-PP/EOR30	1.683 ± 0.392	C-PP/EOR30	2.275 ± 0.747
H-PP/EOR45	4.426 ± 2.232	C-PP/EOR45	2.663 ± 1.065

The important factors that influence the shrinkage of the automotive part are the polymer itself, the processing parameters and morphological properties. The particle size and dispersion of rubber was employed to find the relation of shrinkage and morphology. By the way, it is difficult to find the relation of the shrinkage and particle size of rubber phase due to the differences in orientation of PP/POE blends. Thus, the particle aspect ratio (Table 4.10) was used instead of the particle size [27] in the morphological study. From Figure 4.14 (a, c), %shrinkage on both MD and TD direction decreased with increasing average aspect ratio of extracted rubber of blends [27].

From Table 4.11 and Figure 4.13, the %shrinkage on both MD and TD direction of PP/POE blends decreased with increasing POE content consistent to decreasing %crystallinity of PP/POE blends (section 4.1.7). For comparison of EBR and EOR, the %shrinkage on MD and TD direction of C-PP/EOR (0.47-1.43 % for MD and 0.60-1.46 % for TD) was higher than that of C-PP/EBR blends (0.41-1.40 % for MD and 1.14-1.43 for TD). Conversely, the %shrinkage on MD and TD direction of H-PP/EOR (0.46-1.34 % for MD and 0.66-1.63 % for TD) was lower than that of H-PP/EBR blends (0.53-1.32 % for MD and 0.73-1.58 % for TD). Furthermore, %shrinkage of C-PP/POE was higher than that of H-PP/POE blends on both MD and TD direction, whereas at EBR content of 45wt%, H-PP/EBR45 (0.53 % for MD and 0.73% for TD) showed the higher %shrinkage than C-PP/EBR45 (0.41 % for MD and 0.53% for TD).

Table 4.11 Effect of PP and POE type and blending ratio on % shrinkage of blends

Sample	Shrinkage (%)		Sample	Shrinkage (%)	
	MD	TD		MD	TD
H-PP	1.72 ± 0.05	1.70 ± 0.12	C-PP	1.52 ± 0.02	1.62 ± 0.03
H-PP/EBR15	1.32 ± 0.04	1.58 ± 0.10	C-PP/EBR15	1.40 ± 0.03	1.43 ± 0.03
H-PP/EBR30	0.91 ± 0.02	1.22 ± 0.03	C-PP/EBR30	1.06 ± 0.02	1.14 ± 0.03
H-PP/EBR45	0.53 ± 0.02	0.73 ± 0.02	C-PP/EBR45	0.41 ± 0.02	0.53 ± 0.04
H-PP/EOR15	1.34 ± 0.05	1.63 ± 0.03	C-PP/EOR15	1.43 ± 0.02	1.46 ± 0.02
H-PP/EOR30	0.81 ± 0.04	1.11 ± 0.02	C-PP/EOR30	1.13 ± 0.02	1.20 ± 0.02
H-PP/EOR45	0.46 ± 0.02	0.66 ± 0.04	C-PP/EOR45	0.47 ± 0.01	0.60 ± 0.03

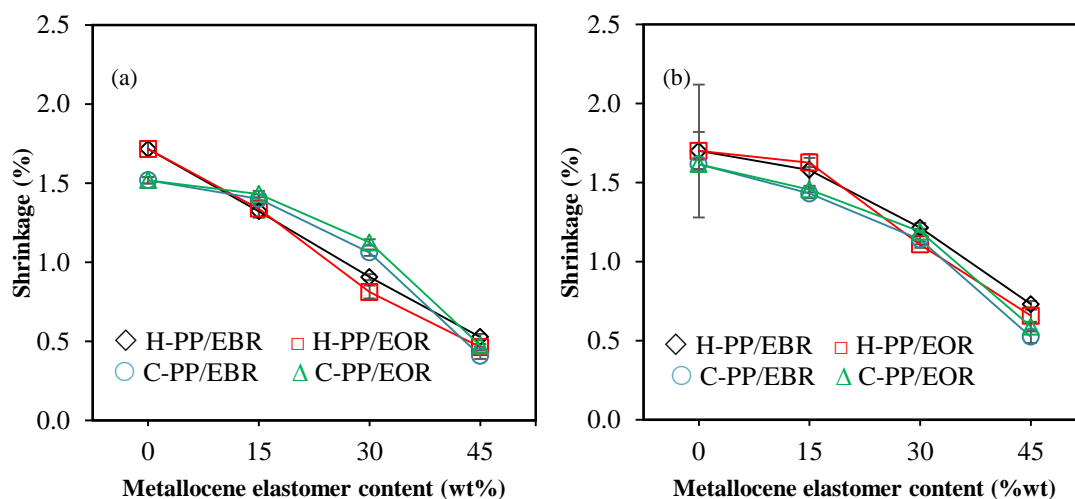


Figure 4.13 Effect of PP and POE type and blending ratio on % shrinkage of blends;
 (a) Machine direction, MD and (b) Transverse machine direction, TD.

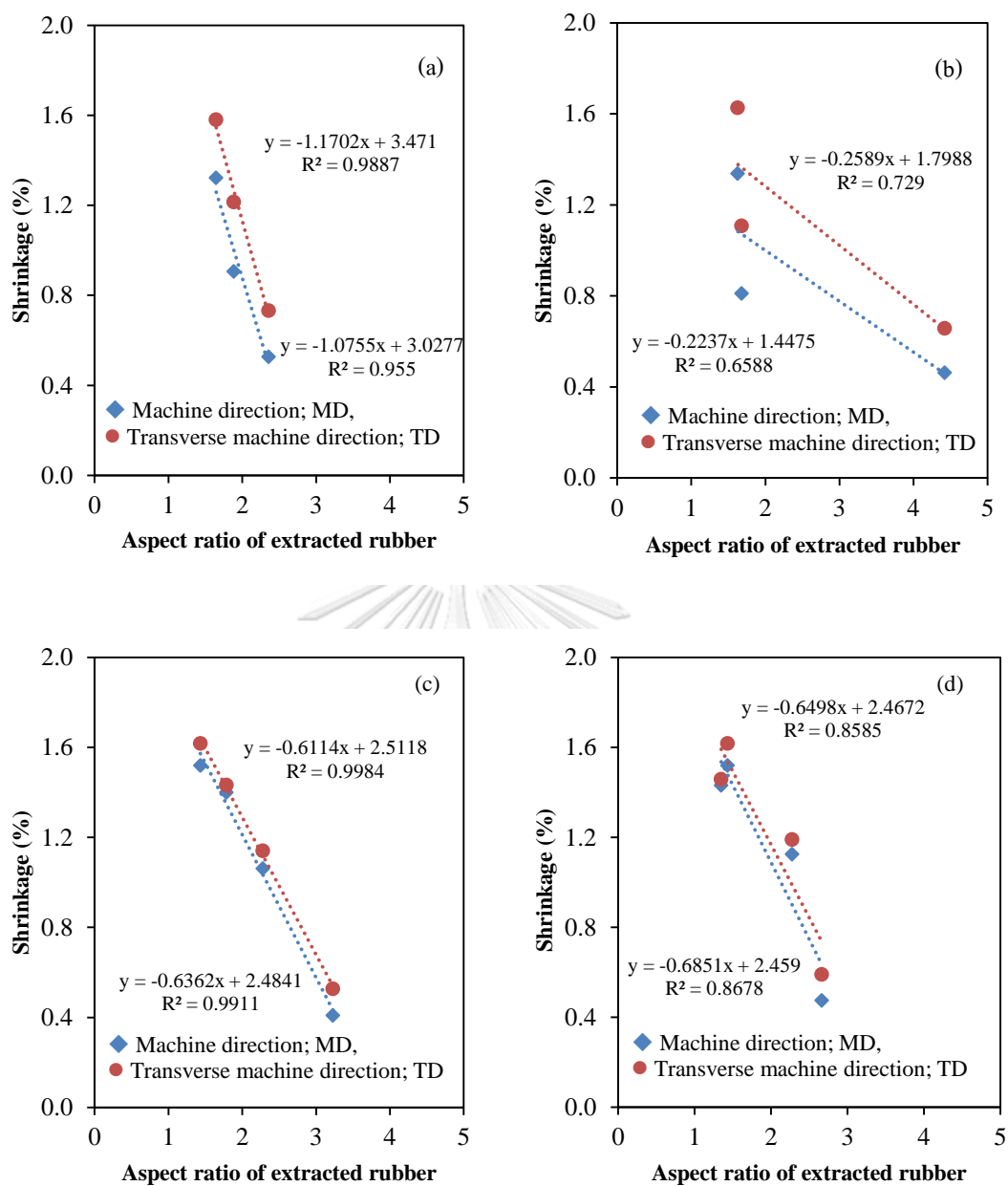


Figure 4.14 The relation of shrinkage and average aspect ratio of extracted rubber of blends; (a) H-PP/EBR, (b) H-PP/EOR, (c) C-PP/EBR, (d) C-PP/EOR.

4.3 Effect of screw speed on physical properties of blends

The H-PP/EOR blends at EOR content of 30 wt% was selected to study the effect of screw speed (400, 500 and 600 rpm) on the physical properties of blends to find the appropriate processing condition for the improved physical properties for automotive application, because the physical properties of H-PP/EOR30 close to the required specification for automotive bumpers. The effect of screw speed on melt flow index, impact properties, tensile properties, flexural properties, shore-d hardness and %crystallinity of the H-PP/EOR30 blends are presented in Table 4.12.

From Figure 4.15 (a), MFI of blend increased slightly with increasing screw speed (400 to 600 rpm). Both Izod and Charpy impact strength at 23°C of H-PP/EOR30 blend extruded at low screw speed (400 rpm) was significantly higher than that of high screw speed (500 and 600 rpm) (Figure 4.15, b-c). Due to the fact that the shear rate increased with increasing screw speed [39] and the high shear rate affected the low entanglement of elastomer chain resulting the higher MFI and lower impact strength of the blends.

From Figure 4.15 (d-f), for the effect of screw speed on blends, the tensile properties and elongation at break of blends did not significantly change. However, tensile modulus of blends was slightly increased with increasing screw speed (400 to 600 rpm). This result can be explained that the increasing screw speed could strengthen the shearing action due to the increasing %crystallinity of blends (from 28.6 to 32.6 %) (Table 4.11). In addition, the flexural properties of H-PP/POE30 blends extruded at 400, 500 and 600 rpm (Figure 4.16, a-b) showed the similar results to the tensile properties [31].

From Figure 4.17 (a-b), T_m and T_c of H-PP/EOR30 blend did not significantly change with increasing screw speed at 400 to 600 rpm (157.7°C for T_m and 127.4-127.6 °C for T_c). However, the ΔH of blend increased with increasing screw speed (59.2 J/g for 400 rpm, 65.9 J/g for 500 rpm and 67.4 J/g for 600 rpm). This can be explained by the similar behavior of the MFI of blend as above discussion (Figure 4.15, a).

Table 4.12 Effect of screw speed on physical properties of blends

Physical properties	Unit	Screw speed (rpm)		
		400	500	600
Melt flow index	g/10min	43.1 ± 0.19	44.0 ± 0.14	45.4 ± 0.18
Tensile strength	MPa	20.6 ± 0.19	21.3 ± 0.26	21.1 ± 0.15
Elongation at break	%	523.3 ± 18.4	514.4 ± 14.2	513.6 ± 14.4
Tensile modulus	MPa	991.1 ± 23.6	1046.1 ± 38.5	1050.6 ± 27.1
Flexural strength	MPa	25.2 ± 0.26	25.8 ± 0.19	25.5 ± 0.15
Flexural modulus	MPa	1096.9 ± 50.8	1100.9 ± 14.8	1118.7 ± 27.0
Hardness (Shore D)	-	58.4 ± 0.19	61.1 ± 0.44	58.4 ± 0.19
Charpy impact strength at 23°C	kJ/m ²	20.7 ± 0.68	19.2 ± 0.69	16.7 ± 0.72
Charpy impact strength at -30°C	kJ/m ²	3.1 ± 0.31	2.9 ± 0.12	2.8 ± 0.07
Izod impact strength at 23°C	kJ/m ²	23.9 ± 0.53	19.2 ± 2.39	18.1 ± 1.81
Izod impact strength at -30°C	kJ/m ²	3.7 ± 0.14	3.7 ± 0.14	3.6 ± 0.28
Heat distortion temperature at 0.45 MPa	°C	82.2 ± 0.76	82.3 ± 1.08	82.7 ± 1.21
Crystallinity	%	28.6	31.8	32.6

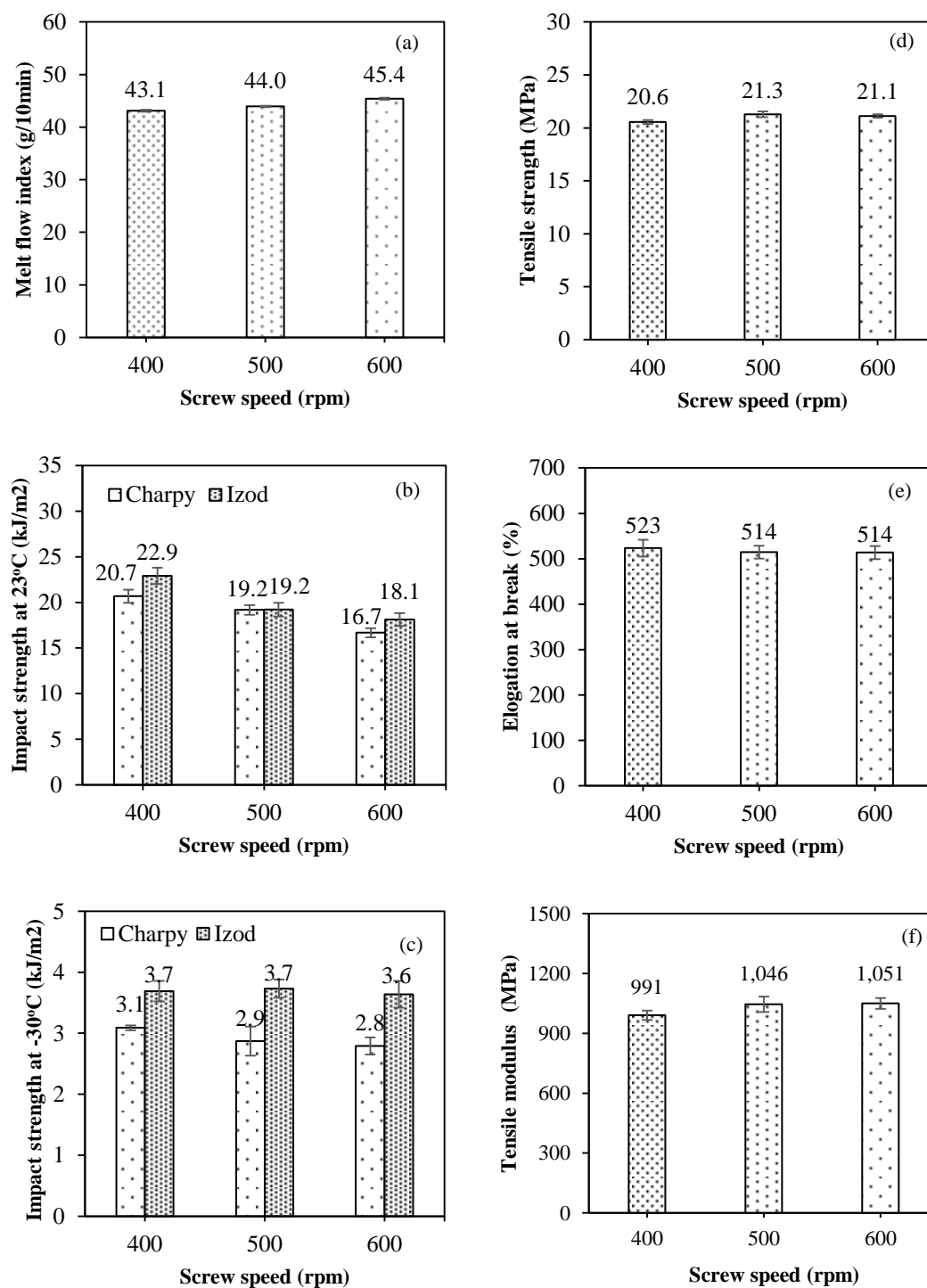


Figure 4.15 Effect of screw speed on physical properties of blends; (a) Melt flow index, (b) Impact strength at 23°C, (c) Impact strength at -30°C, (d) Tensile strength, (e) Elongation at break, (f) Tensile modulus.

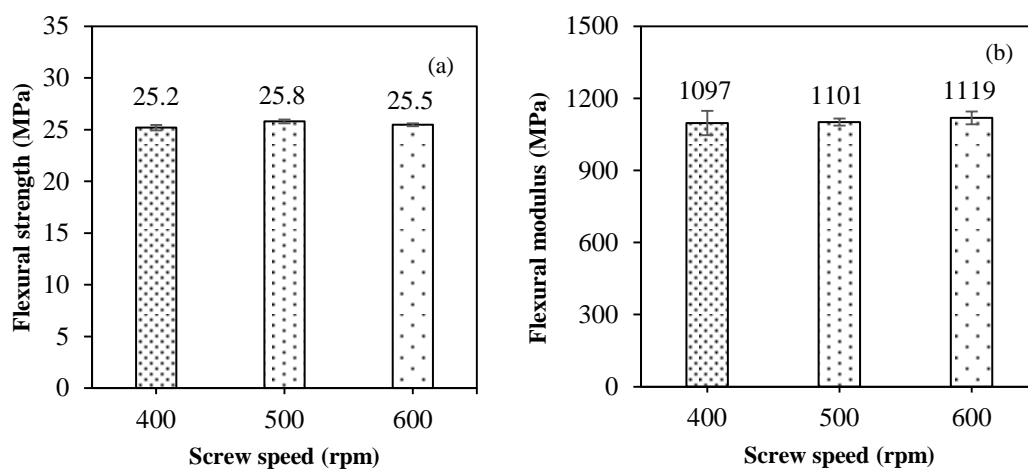


Figure 4.16 Effect of screw speed on flexural properties of blends; (a) Flexural strength, (b) Flexural modulus.

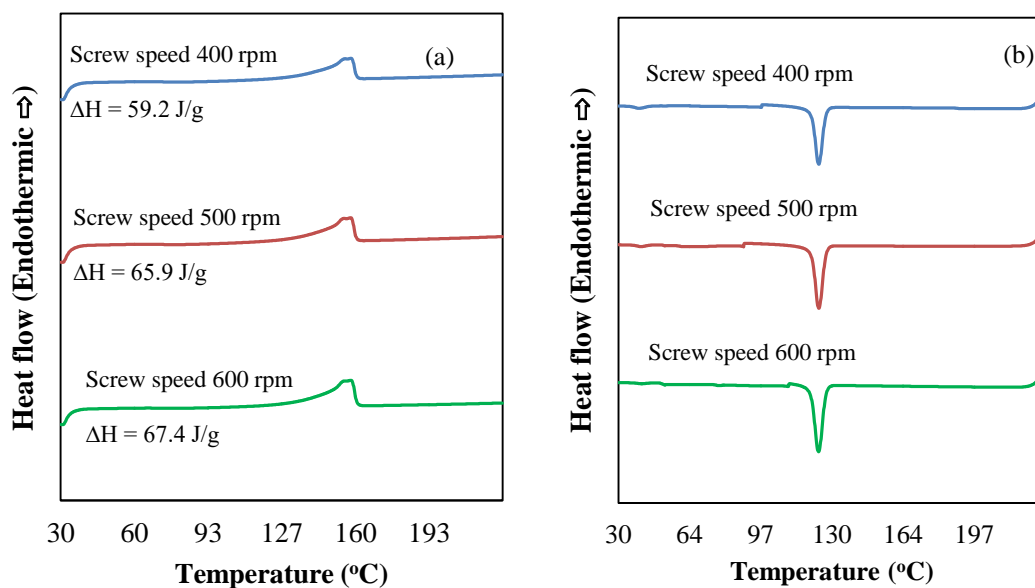


Figure 4.17 DSC thermograms of the H-PP/EOR30 blend; (a) T_m from the second heating scan, (b) T_c from the cooling scan.

4.4 Effect of screw speed on morphological properties of blends

From Figure 4.18 and Table 4.13, the average particle area and average aspect ratio of extracted rubber of blends extruded at 400-600 rpm increased with increasing screw speed. This can be explained that the high screw speed caused the high shear rate leading to the good rubber dispersion. When the particle area or aspect ratio of extracted rubber of blend extruded at high screw speed (600 rpm) was increased resulting the low impact strength [30]. Thus, the elongated dispersed EOR particle was observed in blend extruded at highest screw speed (600 rpm) due to higher share rate by increasing the screw speed [24, 29, 39]. It can be implied that the morphological properties affected the physical properties of H-PP/EOR blends.

The appropriate screw speed was 400 rpm that gave the good physical properties (impact strength, tensile properties and flexural properties) of H-PP/EOR blends.

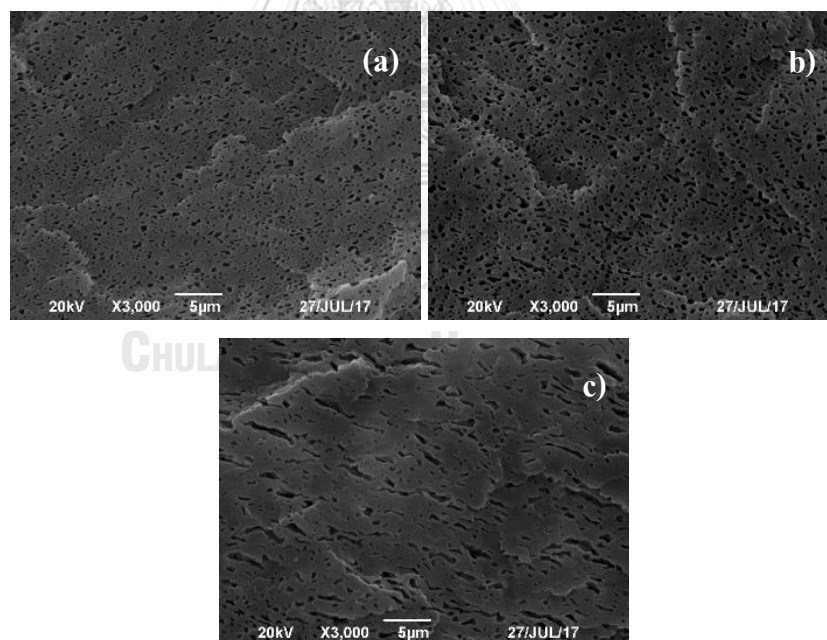


Figure 4.18 SEM micrographs of H-PP/EOR30 at various screw speed; (a) 400, (b) 500, (c) 600 rpm.

Table 4.13 Effect of screw speed on average particle area and aspect ratio of extracted rubber of H- PP/EOC30

Screw speed (rpm)	Average particle area of extracted rubber (μm^2)	Aspect ratio of extracted rubber
400	0.330 ± 0.146	2.079 ± 0.858
500	0.356 ± 0.135	2.275 ± 0.578
600	1.739 ± 0.692	4.064 ± 1.848



4.5 Cost estimation and Benchmarking of PP/POE blends

4.5.1 Cost estimation of blends

The cost estimation was calculated using the raw material price, including H-PP, C-PP, EBR and EOR. In addition, the estimated cost will be used to select the appropriate of blends which is the balance in cost and physical properties. The cost estimation is presented in Table 4.14.

Table 4.14 Summary estimated cost of PP/POE blends

Formulation Name	Cost (baht/kg)	Formulation Name	Cost (baht/kg)
H-PP	42	C-PP	52
H-PP/EBR15	45	C-PP/EBR15	54
H-PP/EBR30	49	C-PP/EBR30	56
H-PP/EBR45	52	C-PP/EBR45	58
H-PP/EOR15	47	C-PP/EOR15	55
H-PP/EOR30	51	C-PP/EOR30	58
H-PP/EOR45	56	C-PP/EOR45	61

Remark: H-PP, C-PP, EBR, and EOR cost are 42, 52, 65 and 72 baht/kg, respectively.

4.5.2 Benchmarking of PP/POE blends

The benchmarking of PP/POE blends was considered using the physical properties compared with the required specification and cost of blends. The benchmarking of PP/POE blends are presented in Table 4.15 and Figure 4.19.

From Table 4.15 and Figure 4.19, four formulations (H-PP/EBR30, H-PP/EOR30, C-PP/EBR15 and C-PP/EOR15) were selected for benchmarking of blends compared with the required specification, because the physical properties of their 4 blends were close to required specification. The best formulation was H-PP/EOR30 blend which gave the good balance of stiffness-impact properties, physical properties and cost. However, the flexural modulus of H-PP/EOR30 blend (1051

MPa) did not meet the required specification (>1200 MPa). Thus, the improved flexural modulus of blend could be further studied.

Table 4.15 Benchmarking of PP/POE blends.

Item	Unit	Specification	H-PP/	H-PP/	C-PP/	C-PP/
			EBR30	EOR30	EBR15	EOR15
Melt flow index	g/10min	39.0	39.2	46.0	48.4	48.3
Tensile strength	MPa	18.0	18.9	21.4	22.8	23.8
Elongation at break	%	>300	>500	>500	44.8	65.6
Flexural strength	MPa	>20.0	23.0	25.8	31.2	31.9
Flexural modulus	MPa	>1200	1013	1051	1289	1318
Charpy impact strength@23°C	kJ/m ²	>13.0	9.0	16.1	10.2	10.8
Charpy impact strength@-30°C	kJ/m ²	>2.0	2.1	2.7	4.9	4.5
Izod impact strength@23°C	kJ/m ²	>13.0	18.3	20.5	10.3	10.7
Izod impact strength@-30°C	kJ/m ²	>2.0	2.8	3.5	5.6	5.5
Cost	baht	-	49	51	54	55

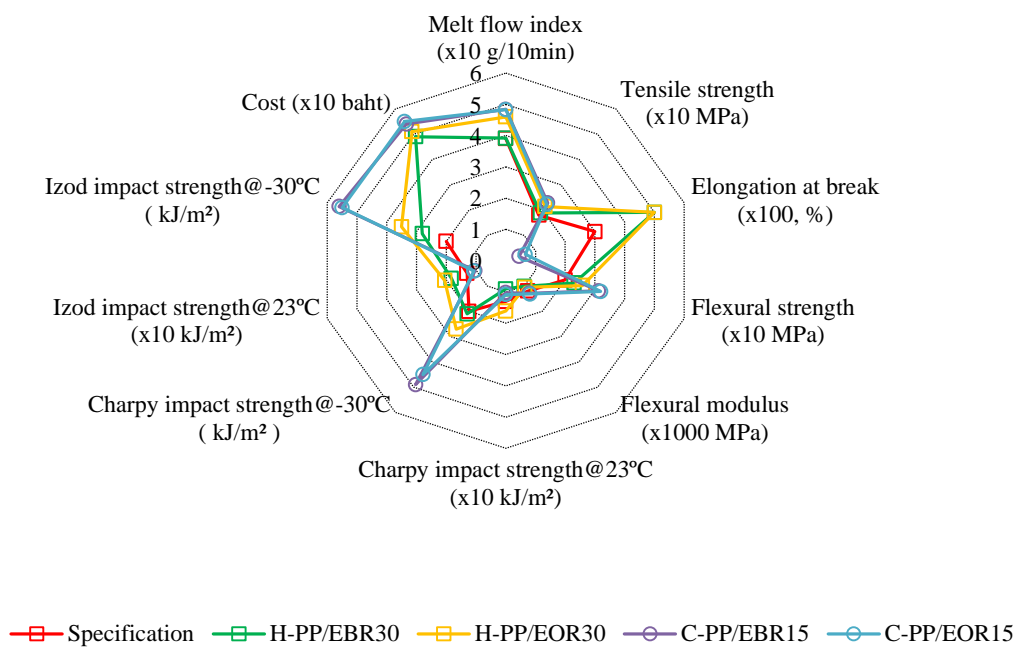


Figure 4.19 Benchmarking of PP/POE blends.



CHARTER V

CONCLUSIONS

5.1 Conclusions

The effects of polypropylene and metallocene elastomer (POE) type, metallocene elastomer (POE) content and screw speed on physical and morphological properties of PP/POE blends were investigated. In this work, the appropriate raw materials, blending ratio and also screw speed of PP/POE blends were obtained for balancing the physical properties especially melt flow index and impact resistance properties for automotive bumpers. The present study could be concluded as follows;

1. The appropriate polymer matrix of PP/POE blends was homopolymer polypropylene (H-PP) and the balance of stiffness-impact properties and physical properties were achieved, especially melt flow index and impact properties.
2. For the metallocene elastomer type, both ethylene butene rubber (EBR) and ethylene octene rubber (EOR) could enhance the impact properties and physical properties. The addition of POE at 30 wt% in PP blends gave the good balance of stiffness-impact properties and physical properties.
3. For the relation of morphology and physical properties, average particle area and aspect ratio of dispersed POE had a pronounced effect on the physical properties of PP/POE blends.
4. The appropriate screw speed was 400 rpm that gave the best physical properties (impact strength, tensile properties and flexural properties) of H-PP/EOR blends.
5. The physical properties, e.g. impact properties of PP/POE blends was affected by the screw speed. Thus, the screw speed could be properly adjusted to achieve the required properties.

5.2 Suggestion for Future Work

1. The properties retention after accelerated weathering should be studied to find the long term stability of PP/POE blends.
2. The effect of talc $[\text{Mg}_3\text{Si}_4\text{O}_{10}(\text{OH})_2]$ or calcium carbonate (CaCO_3) on the physical properties of PP/POE blends should be investigated for the improved flexural modulus.



REFERENCES

1. *Plastics Intelligence Monthly*. 2014; Available from: <http://www.thaiplastics.org>
2. AlMa'adeed, M.A.-A. and I. Krupa, *Polyolefin Compounds and Materials: Fundamentals and Industrial Applications*. 2015: Springer.
3. Paul, G.S., *Polypropylene structure*, in *Polymer Chemistry*. 1963. p. 2317-2325.
4. Mülhaupt, R., *Ziegler-Natta catalysis and propylene polymerization*, in *Polypropylene*. 1999, Springer. p. 896-920.
5. Ewen, J.A., et al., *Propylene polymerizations with group 4 metallocene/alumoxane systems*, in *Transition Metals and Organometallics as Catalysts for Olefin Polymerization*. 1988, Springer. p. 281-289.
6. Corradini, P., *The discovery of isotactic polypropylene and its impact on pure and applied science*. *Journal of Polymer Science Part A: Polymer Chemistry*, 2004. **42**(3): p. 391-395.
7. Haftka, S. and K. Könnecke, *Physical properties of syndiotactic polypropylene*. *Journal of Macromolecular Science, Part B: Physics*, 1991. **30**(4): p. 319-334.
8. Sakata, Y., A. Unwin, and I. Ward, *The structure and mechanical properties of syndiotactic polypropylene*. *Journal of materials science*, 1995. **30**(23): p. 5841-5849.
9. Razavi, A., *Syndiotactic polypropylene: Discovery, development, and industrialization via bridged metallocene catalysts*, in *Polyolefins: 50 years after Ziegler and Natta II*. 2013, Springer. p. 43-116.
10. Koivumäki, J. and J.V. Seppälä, *Comparison of ethylene-propylene copolymers obtained with Ti, V and Zr catalyst systems*. *Polymer Bulletin*, 1993. **31**(4): p. 441-448.
11. Feng, Y. and J. Hay, *The characterisation of random propylene-ethylene copolymer*. *Polymer*, 1998. **39**(25): p. 6589-6596.

12. Tang, W., et al., *Crystallization behavior and mechanical properties of polypropylene random copolymer/poly (ethylene-octene) blends*. Journal of Applied Polymer Science, 2011. **122**(1): p. 461-468.
13. Morton, M., *Rubber technology*. 2013: Springer Science & Business Media.
14. Noordermeer, J.W., *Ethylene-propylene elastomers*. Encyclopedia of Polymer Science and Technology, 2002.
15. Hamielec, A.E. and J.B. Soares, *Metallocene catalyzed polymerization: industrial technology*. Polypropylene: An AZ reference, 1999. **2**: p. 446.
16. Wilczynski, K. and J.L. White, *Melting model for intermeshing counter-rotating twin-screw extruders*. Polymer Engineering & Science, 2003. **43**(10): p. 1715-1726.
17. White, J.L., et al., *Twin screw extruders; development of technology and analysis of flow*. Advances in Polymer Technology, 1987. **7**(3): p. 295-332.
18. Kim, B. and I. Do, *Effect of viscosity ratio, rubber composition, and peroxide/coagent treatment in PP/EPR blends*. Journal of applied polymer science, 1996. **61**(3): p. 439-447.
19. Pukanszky, B., et al., *Effect of multiple morphology on the properties of polypropylene/ethylene-propylene-diene terpolymer blends*. Polymer, 1989. **30**(8): p. 1407-1413.
20. Fortelny, I. and J. Kovář, *Effect of the composition and properties of components on the phase structure of polymer blends*. European polymer journal, 1992. **28**(1): p. 85-90.
21. Bartilla, T., et al., *Physical and chemical changes during the extrusion process*. Advances in Polymer Technology, 1986. **6**(3): p. 339-387.
22. López-Manchado, M.A., et al. *Processing, properties and morphology of polypropylene-epdm blends*. in *Macromolecular Symposia*. 1999. Wiley Online Library.
23. Liu, G. and G. Qiu, *Study on the mechanical and morphological properties of toughened polypropylene blends for automobile bumpers*. Polymer Bulletin, 2013. **70**(3): p. 849-857.

24. Du, H., et al., *Influence of phase morphology and crystalline structure on the toughness of rubber-toughened isotactic polypropylene blends*. *Polymer*, 2014. **55**(19): p. 5001-5012.
25. Kock, C., et al., *Polypropylene/polyethylene blends as models for high-impact propylene-ethylene copolymers, part 1: Interaction between rheology and morphology*. *Journal of Applied Polymer Science*, 2013. **128**(3): p. 1484-1496.
26. Kock, C., et al., *Polypropylene/polyethylene blends as models for high-impact propylene-ethylene copolymers, part 2: Relation between composition and mechanical performance*. *Journal of Applied Polymer Science*, 2013. **130**(1): p. 287-296.
27. Grestenberger, G., G. Potter, and C. Grein, *Polypropylene/ethylene-propylene rubber (PP/EPR) blends for the automotive industry: Basic correlations between EPR-design and shrinkage*. *eXpress Polymer Letters*, 2014. **8**(4).
28. Kazemabad, S.B., et al., *Effects of Blending Sequence on Morphology and Mechanical Properties of Polypropylene/Ethylene-octene Copolymer/Clay Nanocomposites*. 2015.
29. Wu, J.H., et al., *Mechanical properties, morphology, and crystallization behavior of polypropylene/elastomer/talc composites*. *Polymer Composites*, 2015. **36**(1): p. 69-77.
30. Jossé, C., et al., *Elaboration of low viscosity and high impact polypropylene blends through reactive extrusion*. *Polymer Engineering & Science*, 2016. **56**(4): p. 418-426.
31. Farahanchi, A., et al., *The Effect of ultra-high speed twin screw extrusion on ABS/organoclay nanocomposite blend properties*. *Polymer Engineering & Science*, 2017. **57**(1): p. 60-68.
32. Güllü, A., A. Özdemir, and E. Özdemir, *Experimental investigation of the effect of glass fibres on the mechanical properties of polypropylene (PP) and polyamide 6 (PA6) plastics*. *Materials & design*, 2006. **27**(4): p. 316-323.
33. Akande, S., et al., *Assessment of tests for use in process and quality control systems for selective laser sintering of polyamide powders*. *Journal of Materials Processing Technology*, 2016. **229**: p. 549-561.

34. *Polyamide moisture absorption. Relative dimensional change of various nylon products*. 2014; Available from:
<https://knowledge.ulprospector.com/1390/polyamide-moisture-absorption>
35. Lei L., X.D., Hanqing G., Guoying H., *The Effect of SEBS and POE on Properties of Polypropylene*. American Journal of Science and Technology, 2015. **2**: p. 188-194.
36. Lima, P.S., J.M. Oliveira, and V.A.F. Costa, *Partial replacement of EPR by GTR in highly flowable PP/EPR blends: Effects on morphology and mechanical properties*. Journal of Applied Polymer Science, 2015. **132**(22).
37. Dang, B., et al., *Large improvement in trap level and space charge distribution of polypropylene by enhancing the crystalline– amorphous interface effect in blends*. Polymer International, 2016. **65**(4): p. 371-379.
38. Truong, L.T., Å.G. Larsen, and J. Roots, *Morphology, crystalline features, and tensile properties of syndiotactic polypropylene blends*. Journal of Applied Polymer Science, 2017. **134**(12).
39. Yilmazer, U. and M. Cansever, *Effects of processing conditions on the fiber length distribution and mechanical properties of glass fiber reinforced nylon-6*. Polymer composites, 2002. **23**(1): p. 61-71.

Table A-2 Izod impact strength at -30°C of PP/POE blends

Sample / Specimen No.	1	2	3	4	5	6	7	8	Avg	SD.	Min	Max
H-PP	1.6	1.2	1.2	1.2	1.2	1.4	1.2	1.2	1.3	0.13	1.2	1.6
H-PP/EBR15	1.2	1.1	2.3	1.2	1.2	1.3	1.1	1.2	1.3	0.41	1.1	2.3
H-PP/EBR30	2.9	2.8	2.7	2.8	2.7	2.8	2.9	2.7	2.8	0.09	2.7	2.9
H-PP/EBR45	11.0	11.4	9.2	13.2	10.9	11.0	11.2	11.4	11.2	1.08	9.2	13.2
H-PP/EOR15	1.2	1.5	1.4	1.3	1.6	1.6	1.2	1.6	1.4	0.16	1.2	1.6
H-PP/EOR30	3.4	3.8	2.7	3.6	3.8	3.8	3.4	3.6	3.5	0.38	2.7	3.8
H-PP/EOR45	9.6	9.2	9.2	6.8	9.2	10.6	9.9	9.2	9.2	1.10	6.8	10.6
C-PP	3.7	3.7	3.7	3.8	3.9	3.9	3.5	3.5	3.7	0.15	3.5	3.9
C-PP/EBR15	5.3	5.3	5.3	6.0	5.8	6.1	5.3	5.9	5.6	0.34	5.3	6.1
C-PP/EBR30	8.1	8.0	7.9	8.2	8.4	8.1	7.9	8.4	8.1	0.21	7.9	8.4
C-PP/EBR45	59.7	59.8	61.3	61.4	61.6	60.6	59.5	59.9	60.5	0.87	59.5	61.6
C-PP/EOR15	5.8	5.0	4.9	6.3	5.4	5.8	5.9	5.2	5.5	0.48	4.9	6.3
C-PP/EOR30	6.9	7.6	7.2	7.3	7.3	7.4	7.1	7.3	7.3	0.22	6.9	7.6
C-PP/EOR45	61.4	63.7	61.1	61.9	61.2	62.3	61.2	60.9	61.7	0.91	60.9	63.7
H-PP/EOR30 (Screw speed 400 rpm)	3.7	3.7	3.8	4.0	3.6	3.7	3.4	3.7	3.7	0.17	3.4	4.0
H-PP/EOR30 (Screw speed 500 rpm)	3.7	3.7	3.9	3.6	3.8	3.4	3.6	3.7	3.7	0.15	3.4	3.9
H-PP/EOR30 (Screw speed 600 rpm)	3.8	3.5	3.8	3.1	3.8	3.7	3.7	3.7	3.6	0.22	3.1	3.8

Table A-3 Charpy impact strength at 23°C of PP/POE blends

Sample / Specimen No.	1	2	3	4	5	6	7	8	9	10	Avg.	SD.	Min	Max
H-PP	2.3	2.0	2.1	2.1	3.1	2.1	2.2	2.2	2.1	2.1	2.2	0.34	2.0	3.1
H-PP/EBR15	5.4	4.6	4.5	4.8	4.7	2.0	4.7	4.8	4.6	4.9	4.5	0.91	2.0	5.4
H-PP/EBR30	8.5	9.1	10.4	8.9	9.2	9.5	8.5	8.6	8.6	8.7	9.0	0.58	8.5	10.4
H-PP/EBR45	47.9	45.5	40.4	45.5	47.9	46.6	44.1	44.3	44.8	45.5	45.2	2.17	40.4	47.9
H-PP/EOR15	5.2	4.5	4.7	5.3	4.8	4.9	5.4	5.2	5.5	5.5	5.1	0.35	4.5	5.5
H-PP/EOR30	16.3	16.2	17.1	15.2	17.7	16.1	15.6	15.7	15.5	15.8	16.1	0.77	15.2	17.7
H-PP/EOR45	55.4	56.0	53.9	54.0	54.7	55.8	55.2	54.6	55.5	58.9	55.4	1.43	53.9	58.9
C-PP	5.9	5.7	6.0	6.0	6.3	6.2	5.9	6.0	6.0	6.0	6.0	0.16	5.7	6.3
C-PP/EBR15	10.4	10.7	9.6	10.8	10.8	10.6	9.4	10.0	9.8	10.4	10.2	0.51	9.4	10.8
C-PP/EBR30	47.6	47.6	48.4	47.1	48.0	48.0	48.6	47.4	47.4	48.3	47.8	0.51	47.1	48.6
C-PP/EBR45	50.1	52.3	57.8	56.3	51.7	51.9	50.1	51.6	53.4	50.1	52.5	2.62	50.1	57.8
C-PP/EOR15	10.3	10.1	11.4	11.1	11.3	10.3	10.9	11.1	11.2	10.5	10.8	0.49	10.1	11.4
C-PP/EOR30	52.0	53.9	52.9	54.0	53.7	53.6	54.1	52.8	52.7	53.3	53.3	0.70	52.0	54.1
C-PP/EOR45	69.5	68.5	70.3	68.4	67.3	69.7	69.2	68.0	69.7	68.4	68.9	0.93	67.3	70.3
H-PP/EOR30 (Screw speed 400 rpm)	20.6	19.3	21.4	20.6	20.7	20.4	20.5	21.2	22.2	20.6	20.7	0.73	19.3	22.2
H-PP/EOR30 (Screw speed 500 rpm)	19.2	19.0	18.7	18.7	19.1	20.0	19.2	19.1	18.9	20.3	19.2	0.53	18.7	20.3
H-PP/EOR30 (Screw speed 600 rpm)	16.9	17.4	16.9	16.3	16.5	16.3	16.0	16.4	17.0	17.4	16.7	0.50	16.0	17.4

Table A-4 Charpy impact strength at -30°C of PP/POE blends

Sample / Specimen No.	1	2	3	4	5	6	7	8	9	10	Avg.	SD.	Min	Max
H-PP	1.0	1.1	1.1	1.0	1.1	1.0	1.0	1.0	1.0	1.0	1.1	0.03	1.0	1.1
H-PP/EBR15	1.1	1.2	1.1	1.7	1.1	1.2	1.1	1.1	1.4	1.1	1.2	0.19	1.1	1.7
H-PP/EBR30	2.1	2.1	2.1	2.2	2.0	2.1	1.9	2.2	2.1	2.1	2.1	0.09	1.9	2.2
H-PP/EBR45	8.4	9.7	10.7	10.4	10.5	10.0	9.3	9.8	10.6	10.7	10.0	0.75	8.4	10.7
H-PP/EOR15	1.0	1.1	1.5	1.4	1.1	1.1	1.3	1.6	1.1	1.1	1.2	0.21	1.0	1.6
H-PP/EOR30	3.0	2.3	2.5	3.6	2.3	2.7	2.2	2.7	2.9	2.3	2.7	0.43	2.2	3.6
H-PP/EOR45	6.7	7.0	7.4	6.9	6.9	8.4	6.8	7.5	7.8	8.5	7.4	0.63	6.7	8.5
C-PP	2.3	2.3	2.3	2.3	2.2	2.3	2.4	2.4	2.3	2.3	2.3	0.06	2.2	2.4
C-PP/EBR15	5.1	4.9	4.9	4.7	5.0	5.0	4.9	4.9	4.9	5.0	4.9	0.12	4.7	5.1
C-PP/EBR30	8.7	8.3	8.6	8.9	8.4	8.4	8.2	8.1	8.3	8.5	8.4	0.25	8.1	8.9
C-PP/EBR45	73.4	74.3	73.7	73.0	73.1	73.2	71.0	72.6	73.8	72.8	73.1	0.90	71.0	74.3
C-PP/EOR15	4.7	4.7	4.8	4.4	4.4	4.4	4.4	4.5	4.5	4.4	4.5	0.16	4.4	4.8
C-PP/EOR30	6.6	6.3	6.2	6.6	6.7	6.4	6.5	6.3	6.3	6.3	6.4	0.17	6.2	6.7
C-PP/EOR45	59.6	59.8	61.6	64.3	65.0	62.6	61.7	60.4	60.2	61.9	61.7	1.84	59.6	65.0
H-PP/EOR30 (Screw speed 400 rpm)	3.2	3.2	3.2	3.2	3.1	3.1	3.0	3.1	3.1	3.1	3.1	0.04	3.0	3.2
H-PP/EOR30 (Screw speed 500 rpm)	2.9	2.4	2.8	3.0	3.0	2.6	3.1	3.1	3.1	3.1	2.9	0.24	2.4	3.1
H-PP/EOR30 (Screw speed 600 rpm)	2.9	3.1	2.9	2.9	2.8	2.7	2.9	3.1	3.1	3.1	2.9	0.14	2.7	3.1

Table A-5 Tensile strength of PP/POE blends

Sample / Specimen No.	1	2	3	4	5	Avg.	SD.	Min	Max
H-PP	37.0	36.7	36.8	36.7	36.8	36.8	0.10	36.7	37.0
H-PP/EBR15	27.3	27.0	26.8	26.8	28.4	27.3	0.67	26.8	28.4
H-PP/EBR30	19.1	18.7	19.0	19.1	18.8	18.9	0.15	18.7	19.1
H-PP/EBR45	13.6	13.4	13.4	13.4	13.2	13.4	0.16	13.2	13.6
H-PP/EOR15	27.9	28.0	28.0	28.2	28.1	28.0	0.11	27.9	28.2
H-PP/EOR30	21.6	21.6	21.5	21.3	21.2	21.4	0.18	21.2	21.6
H-PP/EOR45	16.4	16.3	16.0	16.0	16.2	16.2	0.19	16.0	16.4
C-PP	31.3	31.2	31.2	31.1	31.0	31.2	0.12	31.0	31.3
C-PP/EBR15	22.9	22.8	22.8	22.8	22.7	22.8	0.06	22.7	22.9
C-PP/EBR30	16.6	16.7	16.5	16.7	16.6	16.6	0.11	16.5	16.7
C-PP/EBR45	12.3	11.9	12.1	11.9	11.9	12.0	0.19	11.9	12.3
C-PP/EOR15	23.8	23.8	23.8	23.8	23.7	23.8	0.05	23.7	23.8
C-PP/EOR30	17.8	17.8	17.7	17.7	17.7	17.7	0.06	17.7	17.8
C-PP/EOR45	14.0	13.9	13.9	13.9	13.8	13.9	0.06	13.8	14.0
H-PP/EOR30 (Screw speed 400 rpm)	20.9	20.5	20.5	20.5	20.5	20.6	0.18	20.5	20.9
H-PP/EOR30 (Screw speed 500 rpm)	21.7	21.1	21.2	21.3	21.1	21.3	0.26	21.1	21.7
H-PP/EOR30 (Screw speed 600 rpm)	21.4	21.1	21.0	21.0	21.1	21.1	0.15	21.0	21.4

Table A-6 %Elongation at break of PP/POE blends

Sample / Specimen No.	1	2	3	4	5	Avg.	SD.	Min	Max
H-PP	29.9	31.1	40.2	34.2	40.6	35.2	5.01	29.9	40.6
H-PP/EBR15	501	518	501	501	508	506	7.38	501	518
H-PP/EBR30	500	503	501	501	503	502	1.34	500	503
H-PP/EBR45	502	502	503	509	502	504	2.92	502	509
H-PP/EOR15	501	501	501	501	501	501	0.21	501	501
H-PP/EOR30	501	501	505	505	504	503	2.11	501	505
H-PP/EOR45	504	501	505	506	501	503	2.15	501	506
C-PP	26.7	28.0	25.7	28.4	28.1	27.4	1.12	25.7	28.4
C-PP/EBR15	42.9	43.1	45.8	49.1	42.9	44.8	2.75	42.9	49.1
C-PP/EBR30	119	92.4	123	118	97.8	110	13.83	92.4	123
C-PP/EBR45	486	478	469	467	476	475	7.69	467	486
C-PP/EOR15	64.6	65.3	67.9	66.0	64.1	65.6	1.48	64.1	67.9
C-PP/EOR30	587	511	511	525	498	526	35.27	498	587
C-PP/EOR45	452	487	470	439	456	461	18.24	439	487
H-PP/EOR30 (Screw speed 400 rpm)	535	518	506	508	549	523	18.36	506	549
H-PP/EOR30 (Screw speed 500 rpm)	534	503	504	506	526	514	14.16	503	534
H-PP/EOR30 (Screw speed 600 rpm)	501	519	503	509	536	514	14.38	501	536

Table A-7 Tensile modulus of PP/POE blends

Sample / Specimen No.	1	2	3	4	5	Avg.	SD.	Min	Max
H-PP	1731.9	1739.2	1692.8	1649.8	1733.5	1709.4	38.09	1649.8	1739.2
H-PP/EBR15	1398.2	1301.6	1360.8	1313.0	1424.1	1359.5	52.87	1301.6	1424.1
H-PP/EBR30	1034.4	1064.3	1000.7	1059.3	1015.2	1034.8	27.48	1000.7	1064.3
H-PP/EBR45	561.4	642.3	595.4	625.7	572.3	599.4	34.37	561.4	642.3
H-PP/EOR15	1322.1	1349.6	1331.5	1321.7	1267.5	1318.5	30.70	1267.5	1349.6
H-PP/EOR30	1094.8	1091.4	1064.5	1075.9	1046.7	1074.7	19.82	1046.7	1094.8
H-PP/EOR45	785.4	795.0	792.2	770.6	771.3	782.9	11.46	770.6	795.0
C-PP	1760.8	1722.4	1694.4	1726.1	1669.8	1714.7	34.44	1669.8	1760.8
C-PP/EBR15	1323.1	1315.7	1283.7	1237.3	1281.1	1288.2	34.03	1237.3	1323.1
C-PP/EBR30	964.2	940.4	972.1	938.1	895.6	942.1	29.87	895.6	972.1
C-PP/EBR45	652.4	612.4	598.9	600.8	643.3	621.6	24.76	598.9	652.4
C-PP/EOR15	1302.6	1374.5	1306.5	1280.2	1303.6	1313.5	35.68	1280.2	1374.5
C-PP/EOR30	962.1	969.5	935.2	905.1	929.3	940.2	26.06	905.1	969.5
C-PP/EOR45	764.8	721.5	712.3	719.8	710.5	725.8	22.31	710.5	764.8
H-PP/EOR30 (Screw speed 400 rpm)	1005.3	984.6	1024.7	967.9	973.2	991.1	23.63	967.9	1024.7
H-PP/EOR30 (Screw speed 500 rpm)	1113.0	1034.7	1025.1	1016.8	1041.0	1046.1	38.51	1016.8	1113.0
H-PP/EOR30 (Screw speed 600 rpm)	1087.3	1058.0	1027.6	1059.9	1020.3	1050.6	27.10	1020.3	1087.3

Table A-8 Flexural strength of PP/POE blends

Sample / Specimen No.	1	2	3	4	5	Avg.	SD.	Min	Max
H-PP	45.1	44.9	45.2	45.7	45.2	45.2	0.32	44.9	45.7
H-PP/EBR15	32.6	32.4	32.7	32.8	34.4	33.0	0.80	32.4	34.4
H-PP/EBR30	23.5	23.0	22.6	23.1	23.0	23.0	0.30	22.6	23.5
H-PP/EBR45	15.2	15.4	15.6	15.5	15.4	15.4	0.12	15.2	15.6
H-PP/EOR15	33.8	33.7	33.9	33.9	33.8	33.8	0.08	33.7	33.9
H-PP/EOR30	25.6	25.7	25.7	26.0	26.0	25.8	0.17	25.6	26.0
H-PP/EOR45	18.1	18.3	18.2	18.9	18.0	18.3	0.34	18.0	18.9
C-PP	43.1	42.9	43.6	43.9	42.9	43.3	0.44	42.9	43.9
C-PP/EBR15	31.1	30.9	31.3	31.6	31.1	31.2	0.28	30.9	31.6
C-PP/EBR30	21.3	20.9	21.3	21.3	21.2	21.2	0.18	20.9	21.3
C-PP/EBR45	13.7	14.0	13.9	14.1	13.6	13.9	0.18	13.6	14.1
C-PP/EOR15	31.8	31.6	32.1	32.2	32.0	31.9	0.24	31.6	32.2
C-PP/EOR30	22.6	22.7	22.7	22.7	22.9	22.7	0.08	22.6	22.9
C-PP/EOR45	15.9	15.9	15.9	15.9	15.7	15.9	0.07	15.7	15.9
H-PP/EOR30 (Screw speed 400 rpm)	25.0	25.3	25.3	25.5	24.8	25.2	0.26	24.8	25.5
H-PP/EOR30 (Screw speed 500 rpm)	25.6	25.9	25.6	26.1	25.7	25.8	0.20	25.6	26.1
H-PP/EOR30 (Screw speed 600 rpm)	25.4	25.7	25.5	25.4	25.3	25.5	0.15	25.3	25.7



Table A-9 Flexural modulus of PP/POE blends

Sample / Specimen No.	1	2	3	4	5	Avg.	SD.	Min	Max
H-PP	1838.3	1700.8	1829.4	1642.7	1698.1	1741.8	87.17	1642.7	1838.3
H-PP/EBR15	1321.0	1334.7	1312.5	1298.0	1318.3	1316.9	13.34	1298.0	1334.7
H-PP/EBR30	1019.1	989.4	1031.0	999.3	1027.5	1013.2	18.17	989.4	1031.0
H-PP/EBR45	640.7	591.3	597.1	609.6	639.6	615.7	23.32	591.3	640.7
H-PP/EOR15	1205.5	1262.9	1318.3	1281.5	1247.1	1263.1	41.73	1205.5	1318.3
H-PP/EOR30	981.7	1035.1	1092.3	1065.8	1080.5	1051.1	44.31	981.7	1092.3
H-PP/EOR45	719.3	733.6	756.3	765.3	732.6	741.4	18.87	719.3	765.3
C-PP	1703.2	1681.0	1748.6	1665.7	1606.2	1680.9	52.20	1606.2	1748.6
C-PP/EBR15	1262.9	1315.2	1359.3	1266.7	1241.1	1289.0	47.68	1241.1	1359.3
C-PP/EBR30	913.7	882.4	875.0	889.2	901.4	892.3	15.40	875.0	913.7
C-PP/EBR45	569.9	599.8	562.3	581.3	555.2	573.7	17.48	555.2	599.8
C-PP/EOR15	1344.1	1281.2	1351.8	1249.8	1365.2	1318.4	50.13	1249.8	1365.2
C-PP/EOR30	921.0	915.4	939.1	840.6	905.2	904.2	37.63	840.6	939.1
C-PP/EOR45	669.3	666.8	701.4	659.2	711.3	681.6	23.15	659.2	711.3
H-PP/EOR30 (Screw speed 400 rpm)	1094.7	1161.5	1092.8	1114.7	1020.7	1096.9	50.76	1020.7	1161.5
H-PP/EOR30 (Screw speed 500 rpm)	1081.4	1119.1	1097.5	1111.5	1095.0	1100.9	14.76	1081.4	1119.1
H-PP/EOR30 (Screw speed 600 rpm)	1102.0	1153.7	1083.5	1131.3	1122.9	1118.7	27.03	1083.5	1153.7

Table A-10 Hardness (Shore-D) of PP/POE blends

Sample / Specimen No.	1	2	3	4	5	Avg.	SD.	Min	Max
H-PP	68.8	68.2	68.5	69.2	69.4	68.8	0.49	68.2	69.4
H-PP/EBR15	66.8	63.8	64.0	64.5	64.8	64.8	1.20	63.8	66.8
H-PP/EBR30	57.8	57.9	57.0	57.5	58.0	57.6	0.40	57.0	58.0
H-PP/EBR45	50.7	50.2	50.9	50.8	50.1	50.5	0.36	50.1	50.9
H-PP/EOR15	65.2	64.8	63.8	64.0	63.1	64.2	0.83	63.1	65.2
H-PP/EOR30	58.7	58.2	58.5	58.3	58.4	58.4	0.19	58.2	58.7
H-PP/EOR45	51.7	54.0	52.6	53.9	52.9	53.0	0.96	51.7	54.0
C-PP	68.3	69.4	69.1	68.7	68.8	68.9	0.42	68.3	69.4
C-PP/EBR15	61.2	62.5	62.8	63.0	63.5	62.6	0.86	61.2	63.5
C-PP/EBR30	57.6	58.7	57.9	58.0	57.2	57.9	0.55	57.2	58.7
C-PP/EBR45	49.0	48.6	48.0	48.5	49.0	48.6	0.41	48.0	49.0
C-PP/EOR15	63.3	63.1	63.1	63.2	64.0	63.3	0.38	63.1	64.0
C-PP/EOR30	59.0	58.8	58.0	57.9	58.5	58.4	0.48	57.9	59.0
C-PP/EOR45	49.7	50.2	50.5	50.3	50.4	50.2	0.31	49.7	50.5
H-PP/EOR30 (Screw speed 400 rpm)	59.6	60.3	59.7	60.3	61.1	60.2	0.60	59.6	61.1
H-PP/EOR30 (Screw speed 500 rpm)	61.4	61.5	60.9	61.2	60.4	61.1	0.44	60.4	61.5
H-PP/EOR30 (Screw speed 600 rpm)	60.9	61.2	60.7	61.2	60.6	60.9	0.28	60.6	61.2

VITA

Mr. Supot Ponhan was born on September 8, 1989 at Muang Nongkhai District, Nongkhai Province. He received his Bachelor's Degree of Science (Industrial Chemistry) at Department of Chemistry, Faculty of Science, King Mongkut's Institute of Technology Ladkrabang in 2013. He began his Master's degree in Petrochemistry and Polymer Science, Program of Petrochemistry and Polymer Science, Faculty of Science, Chulalongkorn University in 2015 and completed his study in December 2017. Presentation: "Polypropylene/Metallocene elastomer blends: Physical and morphological properties" Proceedings of TIChE 2017, Shangri-La hotel, Bangkok, Thailand, October 18-20, 2017.

